

POLITECNICO DI TORINO

**Corso di Laurea Magistrale
in Ingegneria Meccanica**

**Techno-economic and experimental investigation
of waste heat recovery from airplane engines test
benches**



Relatore

Prof. Marco Carlo Masoero

Candidato

Francesca Comaschi

Aprile 2018

List of Contents

List of Contents.....	I
List of Figures.....	IV
List of Tables.....	VII
1 Introduction.....	1
1.1 Context and objective of the project.....	1
1.2 Innovativeness of the project and relevant markets.....	3
2 Techno-economic investigation	4
2.1 Sites description.....	4
2.1.1 Zaventem site	4
2.1.2 Rygge site.....	6
2.2 Investigated solutions.....	7
2.2.1 Boiler solution.....	7
2.2.2 Heat pump solution	8
2.3 Components and models description	10
2.3.1 Recovery heat exchanger	10
2.3.2 Oil loop.....	24
2.3.3 Storage water tank	26
2.3.4 Water loop - boiler case	28
2.3.5 Heating circuit.....	28
2.3.6 Heat pump	29
2.4 Test bench general assumptions for Zaventem site	31
2.4.1 ON-OFF boiler period.....	32
2.4.2 Boiler demand	32
2.5 Test bench general assumptions for Rygge site	37

2.5.1 ON-OFF boiler period.....	37
2.5.2 Boiler demand	38
2.6 Economic aspects	40
2.6.1 Recovery heat exchanger cost.....	41
2.6.2 Oil loop cost.....	41
2.6.3 Storage system cost.....	42
2.6.4 Boiler and water loop cost	42
2.6.5 Heat pump cost	43
2.6.6 Maintenance cost	43
2.6.7 Energy prices	43
2.7 Discussion of the results.....	43
2.7.1 Boiler solution for Zaventem site	43
2.7.2 Boiler solution for Rygge site.....	46
2.7.3 Heat pump solution for Zaventem site	48
2.7.4 Heat pump solution for Rygge site	50
2.8 Payback time.....	50
2.8.1 Boiler solution.....	50
2.8.2 Heat pump solution for Zaventem site	53
3 Experimental investigation.....	54
3.1 Heat exchanger description.....	54
3.2 Test bench description	57
3.2.1 Hot gas generator	59
3.2.2 The mixer	63
3.2.3 Flow straightener.....	64
3.2.4 Ducts.....	66
3.2.5 Chamber	71

3.2.6 Water loop.....	71
3.2.7 Support structures.....	72
3.2.8 Thermal insulation.....	73
3.2.9 Measuring instruments	74
3.3 Experimental results.....	79
3.4 Conclusions.....	89
3.4.1 Techno-economic investigation conclusions.....	89
3.4.2 Experimental investigation conclusions	90
3 Bibliografia.....	91

List of Figures

Figure 1. Zaventem site.	4
Figure 2. Rygge site.....	6
Figure 3. Boiler solution.....	8
Figure 4. Heat pump solution.....	9
Figure 5. Configuration of a test bench.....	11
Figure 6. Pictures of a test bench [4].....	11
Figure 7. Gas temperature along the test bench obtained through CFD calculations.	12
Figure 8. Flow rate repartition.	12
Figure 9. Picture of ACTE’s GAP heat exchanger.....	13
Figure 10. Scheme of the hot gas and of the cold secondary fluid stream inside the GAP heat exchanger.	14
Figure 11. Finned tube heat exchanger operation.....	14
Figure 12. Picture of a finned tube heat exchanger [5].	15
Figure 13. Oil side thermal resistance of ACTE’s recovery heat exchanger - case: turbo fan standard ducts [6].....	17
Figure 14. Gas side thermal resistance of ACTE’s recovery heat exchanger - case: turbo fan standard ducts [6].....	17
Figure 15. Heat transfer rate and pressure drop from the oil side of ACTE’s recovery heat exchanger - case: turbo fan standard ducts [6].....	18
Figure 16. Oil side thermal resistance of ACTE’s recovery heat exchanger - case: turbo jet standard ducts [6].....	18
Figure 17. Gas side thermal resistance of ACTE’s recovery heat exchanger - case: turbo jet standard ducts [6].....	19
Figure 18. Heat transfer rate and pressure drop from the oil side of ACTE’s recovery heat exchanger - case: turbo jet standard ducts [6].....	19
Figure 19. Heat transfer rates evolution during a day - turbo fan standard case with an ACTE recuperator, an oil mass flow rate of 40 [kg/s] and a storage tank volume of 50[m ³]. ...	45
Figure 20. Tank temperature evolution during a week of February.	45
Figure 21. Tank temperature evolution yearly basis.....	46

Figure 22. Heat transfer rates evolution during two weeks - turbo jet standard case with an ACTE recuperator, an oil mass flow rate of 40 [kg/s] and a storage tank volume of 60 [m ³].....	47
Figure 23. Heat transfer rates evolution during a week - turbo fan standard case with an ACTE recuperator, an oil mass flow rate of 40[kg/s], a storage tank volume of 50[m ³] and a <i>Qcdnom</i> of 100 [kW].....	49
Figure 24. Tank temperature and COP estimation.....	49
Figure 25. Payback time parametric study for Zaventem site – turbofan standard with an ACTE recuperator.	51
Figure 26. Installation of the ACTE’s GAP heat exchanger in a chimney [19].	55
Figure 27. Picture of the GAP 50-3-3 heat exchanger [19].	55
Figure 28. Picture of one side of the GAP 50-3-3 heat exchanger [19].....	56
Figure 29. Test bench scheme. 1: centrifugal fan, 2: burner, 3: mixer, 4: flow straightener, 5: converging interface duct, 6: heat exchanger, 7: diverging interface duct, 8: chamber, 9: nozzle bench, 10: discharge duct.	57
Figure 30. Scheme of the hot gas generator.	59
Figure 31. Technical drawing of the hot gas generator layout.	60
Figure 32. Hot air generation unit placed in the room where the test bench has been built.	61
Figure 33. Picture of the burner.	61
Figure 34. Scheme of the new gas line.	62
Figure 35. Pictures of a part of the gas line (left) and the material used for the electric connection (right).	62
Figure 36. Scheme of the mixer design.	63
Figure 37. Picture of one mixing unit.	64
Figure 38. Example illustrating the stabilization length principle.	65
Figure 39. Image of a tube type flow straightener.....	65
Figure 40. Scheme of the design of flow straightener that is implemented in the test bench.	66
Figure 41. Tubes and duct used for the flow straightener construction.	66
Figure 42. Curved duct with turning vanes.	67
Figure 43. Pictures of the curved plates (left) and the finished curved duct (right).....	68

Figure 44. Picture of the transformation duct of ACTE company.	69
Figure 45. Ducts scheme. 1:straight ducts, 2:transformation pieces, 3:particular transformation pieces, 4:curved ducts.....	70
Figure 46. Picture of various ducts used for the test bench construction.	70
Figure 47. Picture of the chamber.	71
Figure 48. Scheme of the type "H" support used to support the second level of the test bench.	72
Figure 49. Image of the material used for the thermal insulation of the ducts (left). Example of the fixation method used (right).	73
Figure 50. Scheme of the nozzle flow meter device [20].	74
Figure 51. Images of the metallic nozzles used and the nozzles attached to the perforated fixation plate.	75
Figure 52. Picture of the perforated plate used as settling mean.	76
Figure 53. Picture of the pressure taps installed.	77
Figure 54. Picture of the absolute pressure sensors.	77
Figure 55. Picture of the differential pressure sensors.	78
Figure 56. Picture of the thermocouples connected to the electronic card.	78
Figure 57. Gas flow rate and temperature tests range.	79
Figure 58. Gas flow rate, temperature range and different water flow rate.	80
Figure 59. Water flow rate and temperature range.	80
Figure 60. Heat transfer rates of the gas and the water side of the GAP heat exchanger.	82
Figure 61. Pressure drops throughout the gas side of the GAP heat exchanger.	84
Figure 62. Pressure drops throughout the water side of the GAP heat exchanger.	84
Figure 63. Efficiency of the water side in function of the gas mass flow rate.	86
Figure 64. Efficiency of the water side in function of the water mass flow rate.	87
Figure 65. Efficiency of the water side in function of the C_{min}	87
Figure 66. Trade of C_{water} and C_{gas} while varying the frequency.	88

List of Tables

Table 1. Inlet conditions for the recovery heat exchanger located in the chimney.	15
Table 2. Effectiveness of both sides of the water tank.	27
Table 3. Heat pump parameters.....	31
Table 4. HDD per months in Brussels [11].....	32
Table 5. Consumed fuel per month in Zaventem site	33
Table 6. Working days per month in Zaventem site.	34
Table 7. Fuel consumption in Zaventem site.....	35
Table 8. Consumed fuel per hour in Zaventem site for a typical January day.	36
Table 9. Number of engines tested per month.	37
Table 10. HDD per months in Rygge [11].	38
Table 11. Fuel consumption in Rygge for the test bench and the preparation room.	39
Table 12. Consumed fuel per hour in Rygge site for a typical January day.	40
Table 13. Cost of the recovery heat exchangers [6].....	41
Table 14. Cost of the oil loop.....	42
Table 15. Energy prices [16] [17] [18].	43
Table 16. Minimum payback times for the boiler solution in Zaventem site.	52
Table 17. Minimum payback times for the boiler solution in Rygge site.....	52
Table 18. Minimum payback times for the heat pump solution in Zaventem site.	53

1 Introduction

1.1 Context and objective of the project

This thesis has been developed at the Thermodynamics Laboratory of the University of Liège, Belgium, under the GREEN project.

The GREEN project, started in 2011, is a partnership between the University of Liège and different companies with the purpose of finding solutions to recover energy from airplane engines that are tested in appropriate test benches. The aim of the project is the application of existing technologies and techniques, which are used in other industrial sectors, to the aerospace test sector.

An important aspect of this project is the possibility to reduce the gas emissions in the atmosphere. The European Union (EU) has set a 20% energy saving target for 2020 (compared to 1990) and a dedicated directive on Energy Efficiency to define a set of constraining measures to help European countries reach it [1]. Furthermore, on 30 November 2016 the European Commission proposed an update to the Energy Efficiency Directive, including a new 30% energy efficiency target for 2030. Following these directives, capturing and converting heat losses into electricity or using them for heating purpose, is currently arousing much attention. This allows to reduce not only the thermal pollution, due to the direct release of hot gas into the environment, but also to reduce the fuel expenditure of the airplane engines test benches close buildings and so to reduce their emissions [2]. The hot exhaust gas contains a large quantity of pollutants CO₂, NO_x, Sox etc. which are responsible for environmental harmful impacts such as global warming, acid rain etc. [3].

The airplane engines are tested for several reasons:

- in the development phase of a new model
- to check if an engine works properly at the end of the production
- to verify the repair after maintenance.

The test benches allow to test four types of airplane engines: turbojet, turbofan, turboprop and turboshaft.

Particularly, the main topic of this study is the waste heat recovery, considering various technological solutions. The waste heat comes from the hot exhaust gas. The recovered energy could be used for different purposes such as heating some close buildings or generating electricity, it depends on the solution adopted and on the conditions of the exhaust gas mass flow. However, only the heating purposes have been considered in this thesis. The facilities where the test benches are installed, count with buildings that need to be heated to achieve a comfortable room temperature. The main goal of the WHR (Waste Heat Recovery) systems for heating purposes is to recover part of the thermal energy from the exhaust gas and to use it to cover the heating demand of the buildings, or at least a part of it. Since a part of the energy that will be used for heating comes from a heat source that is “free”, currently the thermal energy of the exhaust gas is wasted, the costs related to the heating of the different buildings will decrease.

The dissertation is organised in two chapters: the first one is a techno-economic investigation and the second one is an experimental investigation.

The first section intends to give the perspectives about the feasibility of including a waste heat recovery system in two aeronautic engine test benches located in Zaventem (Belgium) and in Rygge (Norway). A techno-economic study of the two test benches has been carried out, according to the options investigated that will be shown subsequently. In order to assess the opportunity of incorporating a waste heat recovery system and the convenience, economics aspects such as estimations of the investment costs and the payback time were taken into account.

In the second part, the experimental section, a new type of recovery heat exchanger, which could be used to recover energy from the hot exhaust gas, has been tested in order to verify its performance. This heat exchanger may will be the subject of future other techno-economic studies.

The main partner companies of the GREEN project are:

- CENCO: is a business unit of Techspace Aero (Safran Group), specialized in the design, manufacture, installation, and maintenance of test benches for aerospace engines.
- ACTE: heat exchanger designer and manufacturer company.

The waste heat recovery systems were modelled with EES (Engineering Equation Solver), so all the calculations and graphs of the first part have been obtained with this software.

1.2 Innovativeness of the project and relevant markets

Airplane engines test benches are large consumers of fuel. The fuel consumption can get to some thousands of liters per hour when huge engines are tested.

Obviously, it is not possible to reduce or to avoid the tests since these are essential for the safety of air transport.

The GREEN project provides the real possibility of developing waste energy recovery systems for airplane engines test benches. Considering the large quantities of fuel consumed, even if only a little part of it may be recovered, the consequences can be considerable for the test sites for example for the limitation of the energy consumption (heat and electricity) which directly generates a financial gain and improves the environmental impact.

Nowadays, around the world there are not test benches equipped with specific waste energy recovery system. That is why the project is considered completely innovative.

CENCO is a leader company in the building sector of airplane engines test benches. CENCO, with the GREEN project, would like to take the lead on these new solutions in order to have a technical advantage over the competitors supply.

Aeronautic test benches shall be used by different types of customers:

- OEM (Original Equipment Manufacturers) or engine manufacturers. They use the test benches for developmental and production purposes. Each engine is carefully tested before assembling it on the airplanes. The main engine manufacturers are for example: Pratt & Whitney, General Electric Company, Rolls-Royce and others.
- MRO (Maintenance, Repair and Overhaul) or maintenance centres. They perform engines maintenance tests on behalf of third parties. These maintenance centres are for example: Rolls-Royce, MTU, Snecma.
- Airline companies that choose to do the engines maintenance domestically as Air France or Air China.

- The armies that choose to do the engines maintenance domestically to remain independent in case of conflict, for example the Belgian, the French and the Pakistani armies.

The test benches, integrated with the additional recovery systems developed in the GREEN project, are intended for the four types of customers. However, the profitability of the systems would be higher for long and repeated tests, so for OEM, MRO and big Airline companies.

2 Techno-economic investigation

2.1 Sites description

This section summarizes information about the two investigated sites given by CENCO to carry out the techno-economic simulation.

2.1.1 Zaventem site



Figure 1. Zaventem site.

Zaventem's test bench is located in the airport area of Brussels and is usually used for the maintenance of turbofan civil engines. In 2016, it was also used to develop a new kind of turbofan engine.

Types of tested engines:

- CFMI CFM-56-3
- CFMI CFM56-7B
- CFMI LEAP (development in 2016)

Location:

Europe, Belgium, Zaventem

Year of data for building consumption and test hours:

2016

Hours of tests for 2016:

The amount of test hours during 2016 ranges from 700 to 755 hours.

Fuel consumption for heating need:

The existing boiler fuel consumption to heat buildings near the test bench is 40000 $\left[\frac{l}{year}\right]$.

The boiler is turned on from October to May.

2.1.2 Rygge site



Figure 2. Rygge site.

Rygge test bench is located in the airport area of Rygge in Norway and is usually used for the maintenance of military turbojet engines.

Types of tested engines:

Pratt & Whitney F100-220

Location:

Europe, Norway, Rygge

Year of data for building consumption and test hours:

2016

Hours of tests for 2016:

29 motors have been tested during 2016 (110000 liters of fuel consumed). A test duration is comprised between 4 and 6 hours.

Fuel consumption for heating need:

The LPG (propane) boiler consumed about 10000 kg during the year for the test bench and the preparation room. The same boiler is also used to heat a neighboring storage building at 8 [°C] to 10 [°C] during cold periods. It is consumed 5000 [kg] more over the year to perform this task. In total, the LPG consumption is 15000 [kg] per year for the test bench, the preparation room and the neighboring storage building.

2.2 Investigated solutions

Results from previous studies have shown that the turbofan, turboprop and turboshaft test benches do not represent an attractive alternative to produce electrical power, because of their low return on investment.

However, many commercial airplanes use the turbofan type engine as propulsion device. For this reason, the turbofan test benches are the ones with the higher commercial success. Due to the fact that the turbofan test benches have the higher demand and are also the most sold units, the waste heat recovery study for heating purposes has been performed. The exhaust gas from the turbofan test benches represents the heat source.

In the same way, the waste heat recovery study for heating purposes has been performed for turbojet engine test bench, because they also represent a free heat source.

The two different case studies investigated in this thesis are:

1. WHR for heating purposes: **BOILER SOLUTION**
2. WHR for heating purposes: **HEAT PUMP SOLUTION**

In both cases the use of a water tank, in order to store the energy recovered from the exhaust gas, has been considered because the tests are performed only during specific hours and days.

Furthermore, the heat pump solution has proved to be not feasible, during the study, for turbojet engines.

2.2.1 Boiler solution

Figure 3 shows a schematic representation of the boiler solution.

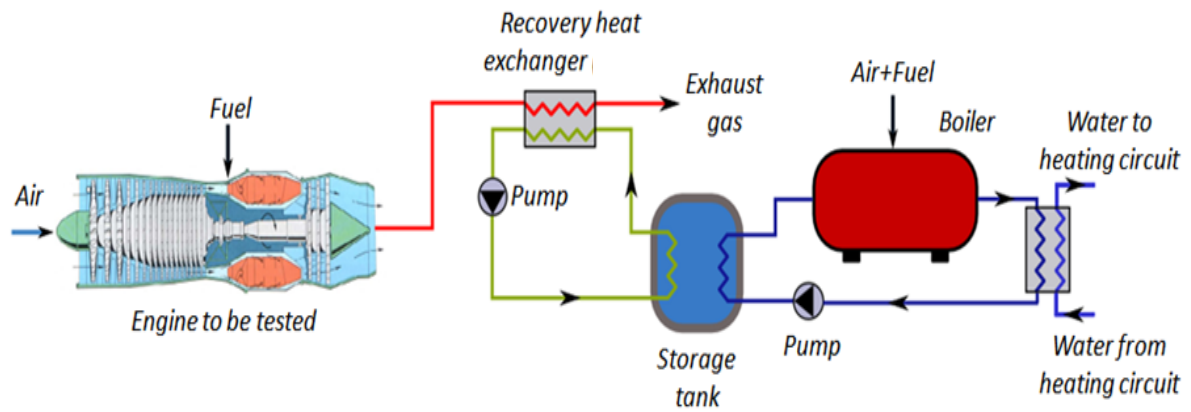


Figure 3. Boiler solution.

The first option is to use the recovered heat, as the preheating of the fluid that is being heated by a preexisting boiler.

The heat in the recovery heat exchanger is transferred firstly to another fluid, oil in this case, and then to a storage tank. The hot fluid (water) contained in the tank is used to preheat the water that is going to be heated by the boiler. In this way, since the fluid is already preheated, the boiler needs to deliver less power, to achieve the desired temperature of the heating circuit. Less power means less fuel and so a lower cost and it also means lower emissions.

2.2.2 Heat pump solution

One alternative to heat the facilities from the test center is the use of a heat pump. A heat pump is a device that is able to provide heat from a heat source to a heat sink. The heat pump uses a refrigerant that is compressed to increase its temperature on the side that has to be warmed. The refrigerant in its gaseous state is compressed by means of a compressor. Then, the refrigerant at high pressure and temperature releases heat at the condenser until it condensates. The condensed refrigerant passes through an expansion valve that reduces its pressure. Afterwards, the low-pressure liquid absorbs heat and change from a liquid to a gaseous state in the evaporator. Then the refrigerant returns to the compressor and the cycle is repeated.

The recovery heat exchanger is used to recover heat from the exhaust gas stream. Then the heat is transferred to a storage tank. The hot fluid contained in the tank is used as heat source for the heat pump (when the tests are and are not running) and the heat is transferred to the water system of the buildings heating system at the condenser. The current boiler is used as a back-up boiler in order to provide the right amount of heat to the building if the heat pump is not powerful enough, or to provide the entire heating need i.e. if the heat pump performance is too small, inferior to a COP of 2.5.

Figure 4 shows a schematic representation of the heat pump solution:

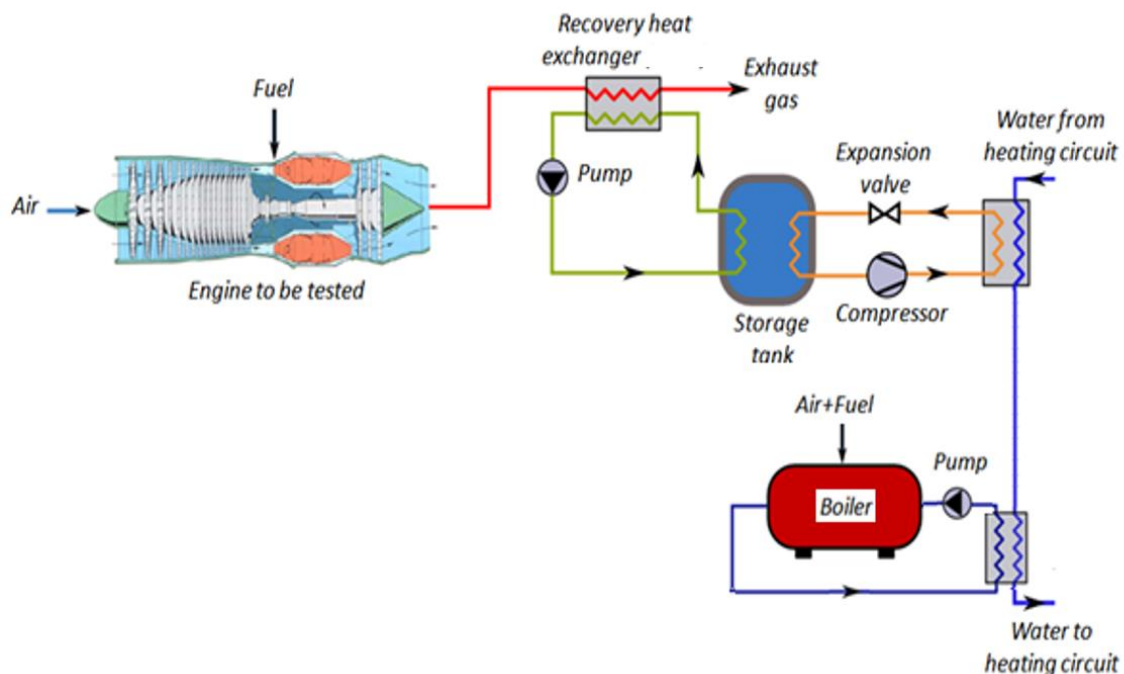


Figure 4. Heat pump solution.

2.3 Components and models description

All the components have been modelled on EES (Engineering Equation Solver)

2.3.1 Recovery heat exchanger

In each of the two studied solutions, the main part is represented by the recovery heat exchanger, which works with the exhaust gas mass flow and a secondary fluid.

Two different kinds of heat exchangers are investigated in this study:

- **ACTE prototype** (also called, “GAP heat exchanger”)
- **Finned tube**

The finned tube heat exchanger has been also considered in this study in order to make a comparison between ACTE prototype and the most popular and widespread technology present in the market. The information, data and technical specifications of the heat exchangers have been provided by ACTE company, partner in this project.

Two potential locations of the heat exchanger should be considered:

- heat exchanger located at the periphery of the augmentor tube,
- heat exchanger located in the chimney, before the acoustic baffles.

The first option has been excluded, because previous studies showed that this solution was not efficient. The large cross section and available space that exist in the test bench chimneys allows the use of bigger heat exchangers that can recover a high amount of heat. Also, the pressure drops are smaller in the recovery heat exchanger due to a large cross section. If the pressure drops were too high, the results concerning the engine performance obtained during an on-going test would be affected.

Figure 5 shows the configuration of a test bench and figure 6 shows some pictures of a test bench.

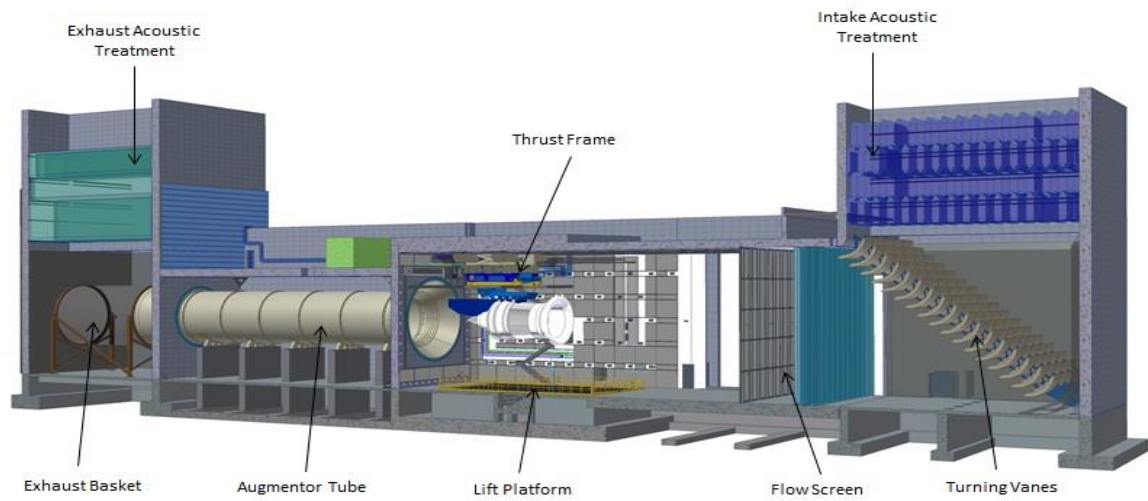


Figure 5. Configuration of a test bench.

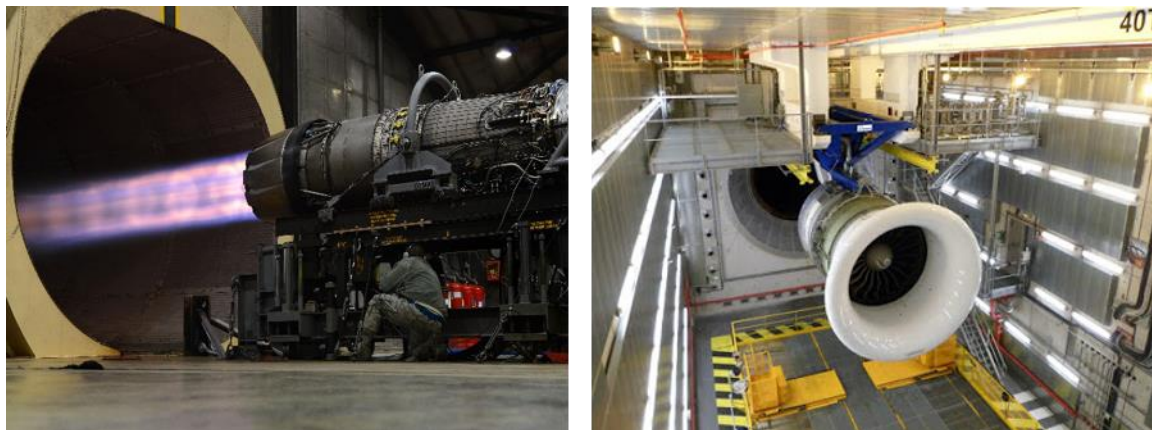


Figure 6. Pictures of a test bench [4].

Furthermore, the heat exchanger should be installed on the right side of the chimney, because most of the hot gas flow goes there as can be seen in figure 7.

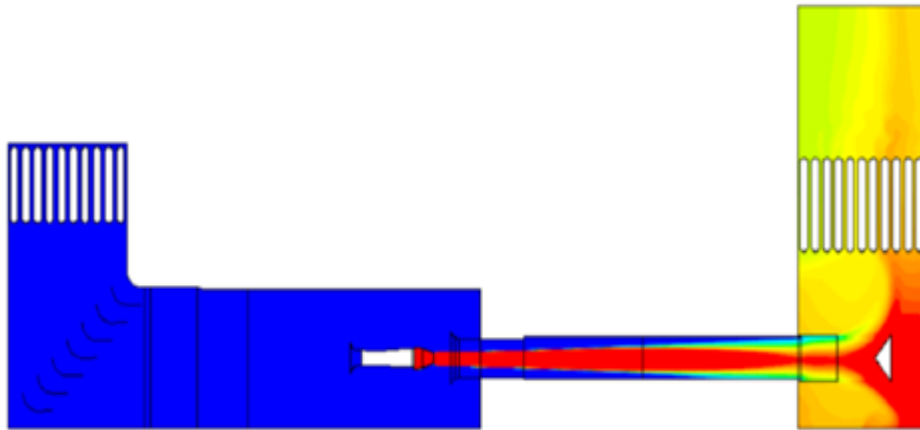


Figure 7. Gas temperature along the test bench obtained through CFD calculations.

It is worth mentioning that, in the chimney, not all the exhaust gas flow crosses the heat exchanger. Some CENCO's studies have shown that around half of the gas flow crosses it. The other half by-passes the heat exchanger. Figure 8 shows the distribution of the flow rate.

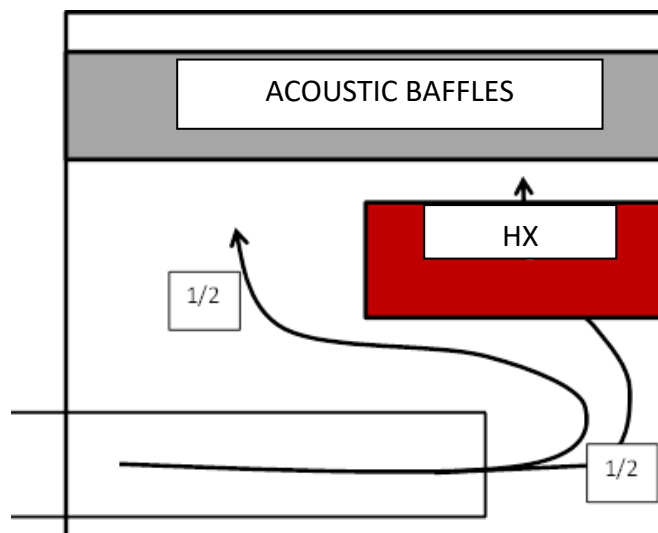


Figure 8. Flow rate repartition.

The description of the two heat exchangers considered in this study is given below.

ACTE's GAP technology has been developed to recover heat from the hot waste gas released during existing industrial processes without impacting the process itself. Figure 9 shows a picture of the rectangular counter-current GAP heat exchanger.

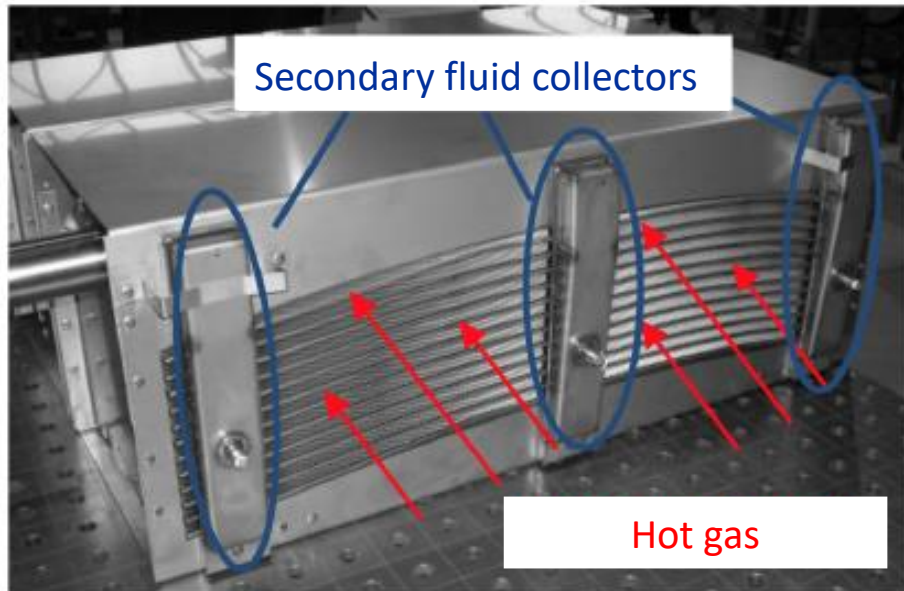


Figure 9. Picture of ACTE's GAP heat exchanger.

In the GAP heat exchanger, the heat exchange surface is optimized. ACTE's GAP heat exchanger is manufactured using a clever mix of pipes and plates, allowing a closed volume in which the secondary liquid can flow and providing a much larger exchange surface. The secondary liquid flows through the tubular plates. It is distributed at the inlet and recovered at the outlet by collectors. Figure 10 shows the process inside the GAP heat exchanger.

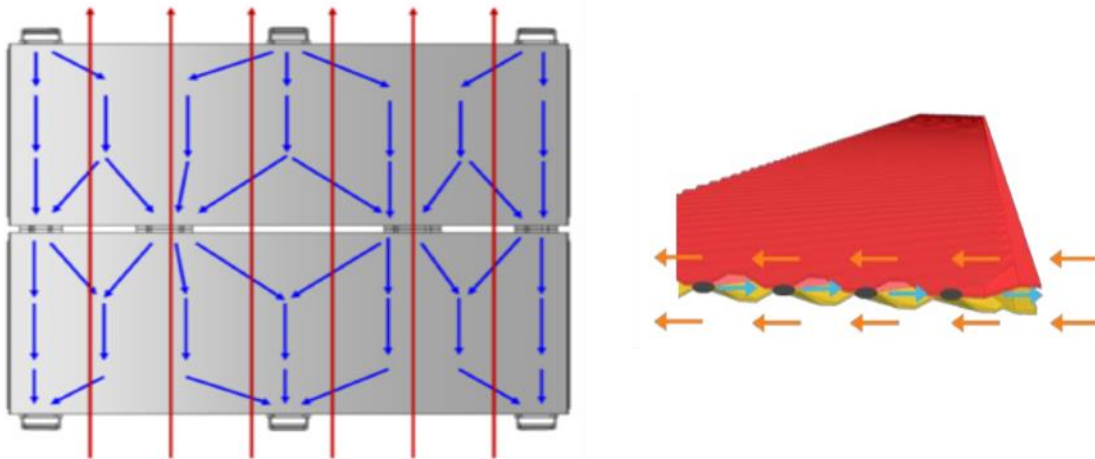


Figure 10. Scheme of the hot gas and of the cold secondary fluid stream inside the GAP heat exchanger.

The finned tube heat exchanger consists of tubes with extended outer surface area in order to increase the heat transfer rate from the additional area of fins. It's possible to understand the finned tube heat exchanger operation from figure 11.

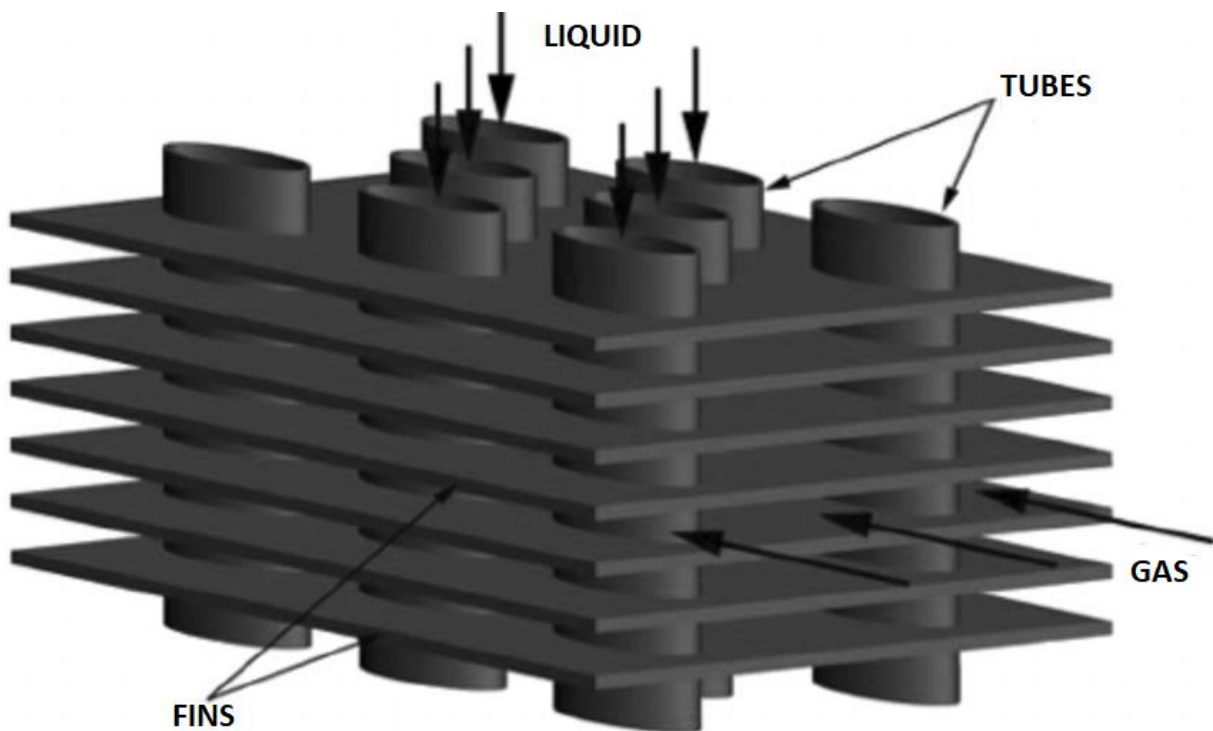


Figure 11. Finned tube heat exchanger operation.



Figure 12. Picture of a finned tube heat exchanger [5].

2.3.1.1 Recovery heat exchanger gas inlet conditions

The inputs of the model for each of the engine test benches have been provided by CENCO. Table 1 shows the conditions of the exhaust gas entering in the recovery heat exchanger for the different test benches. These values are used as inputs to develop the recovery heat exchanger model and to perform the thermal simulations. The ducts' layout of the test benches could be standard or enlarged.

Table 1. Inlet conditions for the recovery heat exchanger located in the chimney.

Test Bench type	Type of duct	Exhaust gas mass flow [kg/s]	Exhaust gas temperature [°C]
Turbofan	Standard	620	61
Turbofan	Enlarged	726,5	55
Turbojet	Standard	276	298
Turbojet	Enlarged	275,5	299

The mass flows and temperatures from Table 1 are considered as the ones existing when the test bench operates at full load.

Both cases of the ducts' layout are considered for the test benches in Zaventem and in Rygge.

2.3.1.2 Simplified model of the recovery heat exchangers

Regarding the GAP heat exchanger, due to the confidentiality of the internal sizing model used by ACTE, the amount of information about ACTE's recovery heat exchanger (heat transfer coefficient correlations, pressure drop correlations, etc.) that they are able to share openly is quite restricted. This missing information is essential to develop a good heat exchanger model. Nevertheless, as a solution, ACTE provided curves and extrapolated correlations of results obtained with their internal heat exchanger model, for each case. The information provided by the mentioned curves and laws is: the value of the thermal resistance of the gas side of the recovery heat exchanger, in function of the gas mass flow rate, and the values of the thermal resistance, the heat transfer rate and pressure drop from the oil side of the recovery heat exchanger, in function of the oil mass flow rate. Curves provided by ACTE have been approximated with polynomial laws in order to develop a simplified recovery heat exchanger model and to be less heavy for the EES calculation performed. The figures below show a comparison between the polynomial law (red or green curve) and the original one (black and blue curve) for turbofan and turbojet engines for standard ducts' layout.

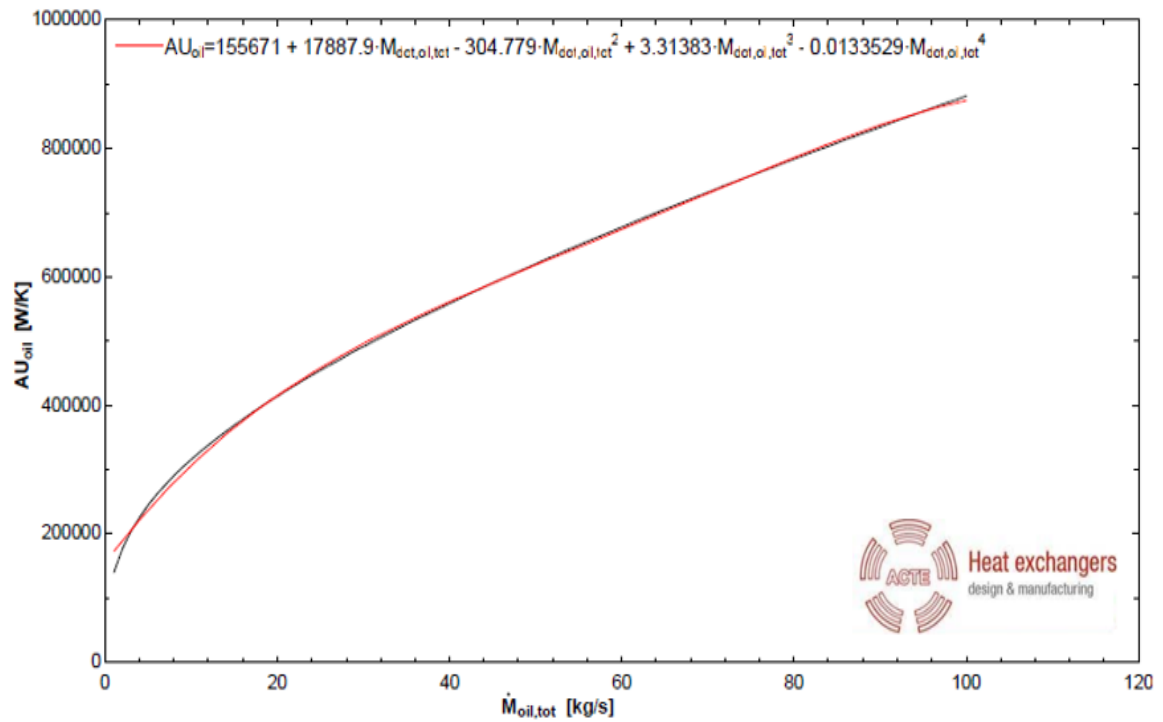


Figure 13. Oil side thermal resistance of ACTE's recovery heat exchanger - case: turbo fan standard ducts [6].

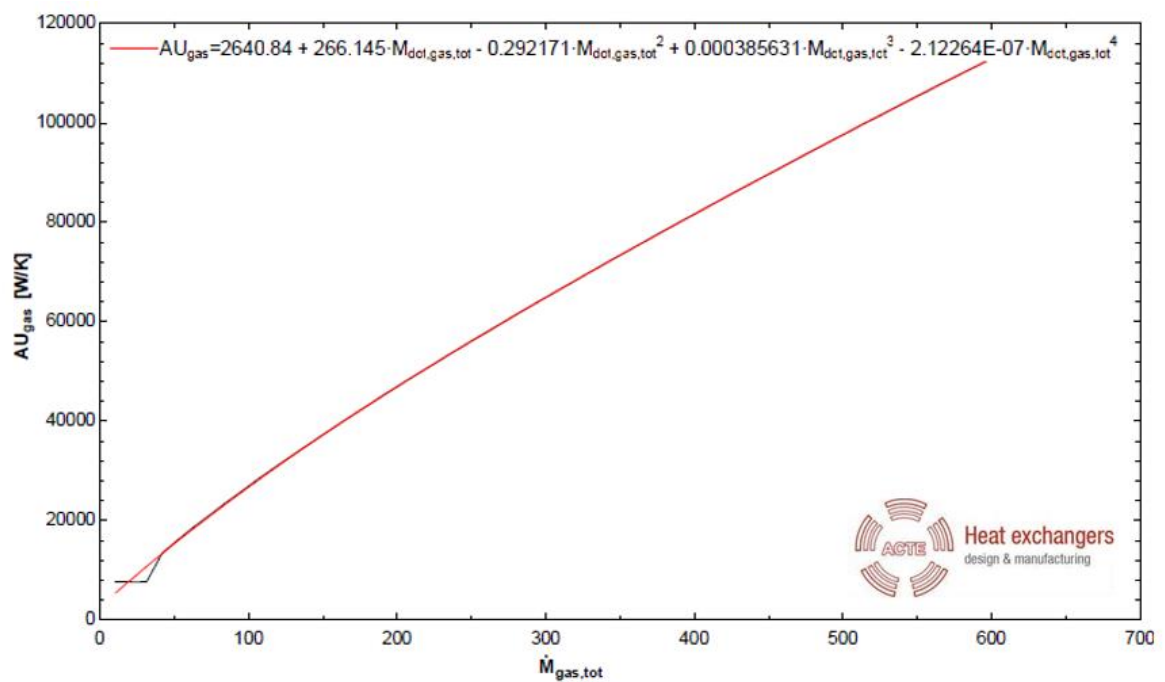


Figure 14. Gas side thermal resistance of ACTE's recovery heat exchanger - case: turbo fan standard ducts [6].

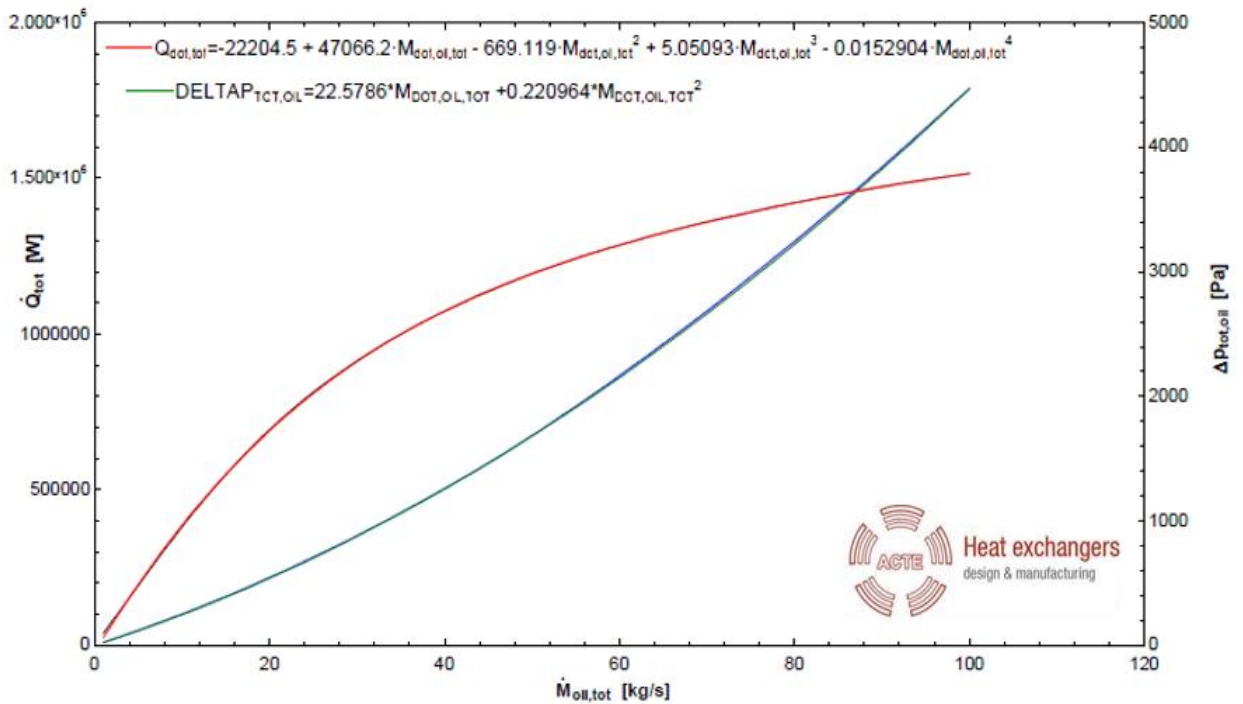


Figure 15. Heat transfer rate and pressure drop from the oil side of ACTE’s recovery heat exchanger - case: turbo fan standard ducts [6].

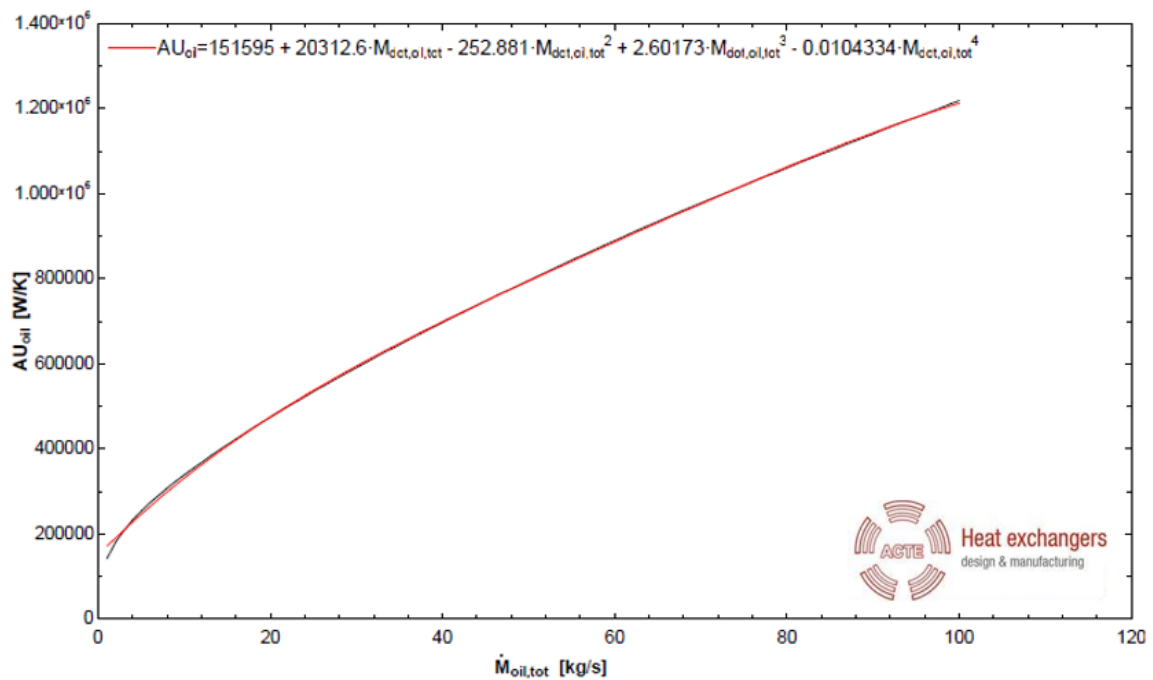


Figure 16. Oil side thermal resistance of ACTE’s recovery heat exchanger - case: turbo jet standard ducts [6].

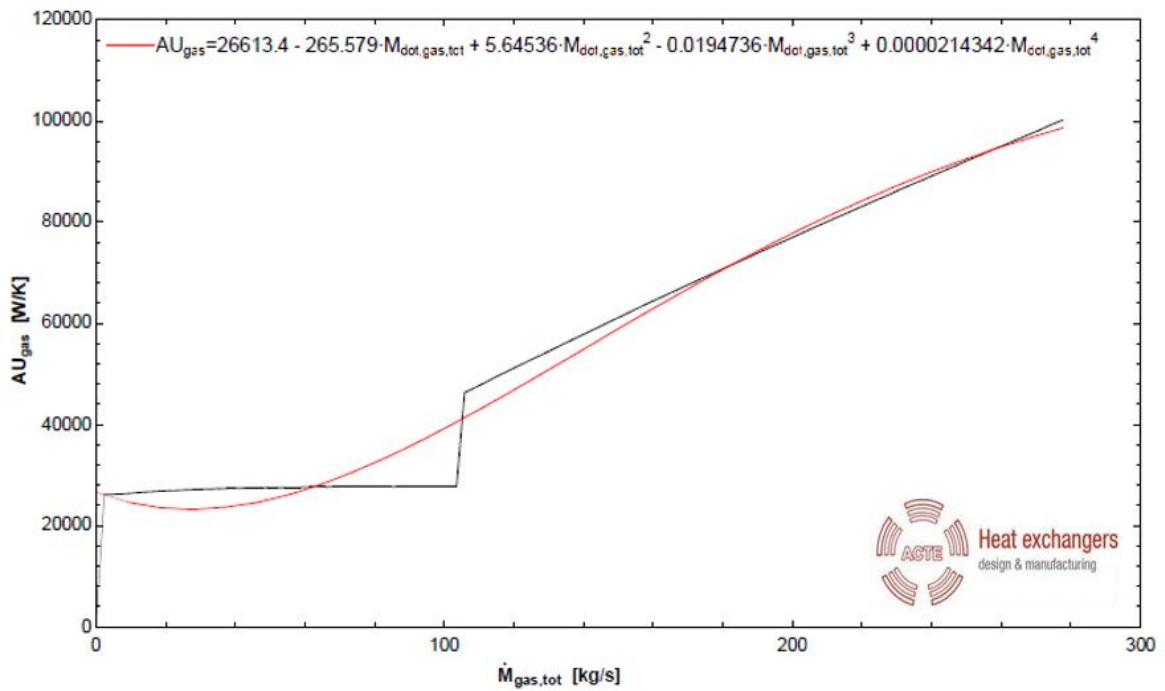


Figure 17. Gas side thermal resistance of ACTE's recovery heat exchanger - case: turbo jet standard ducts [6].

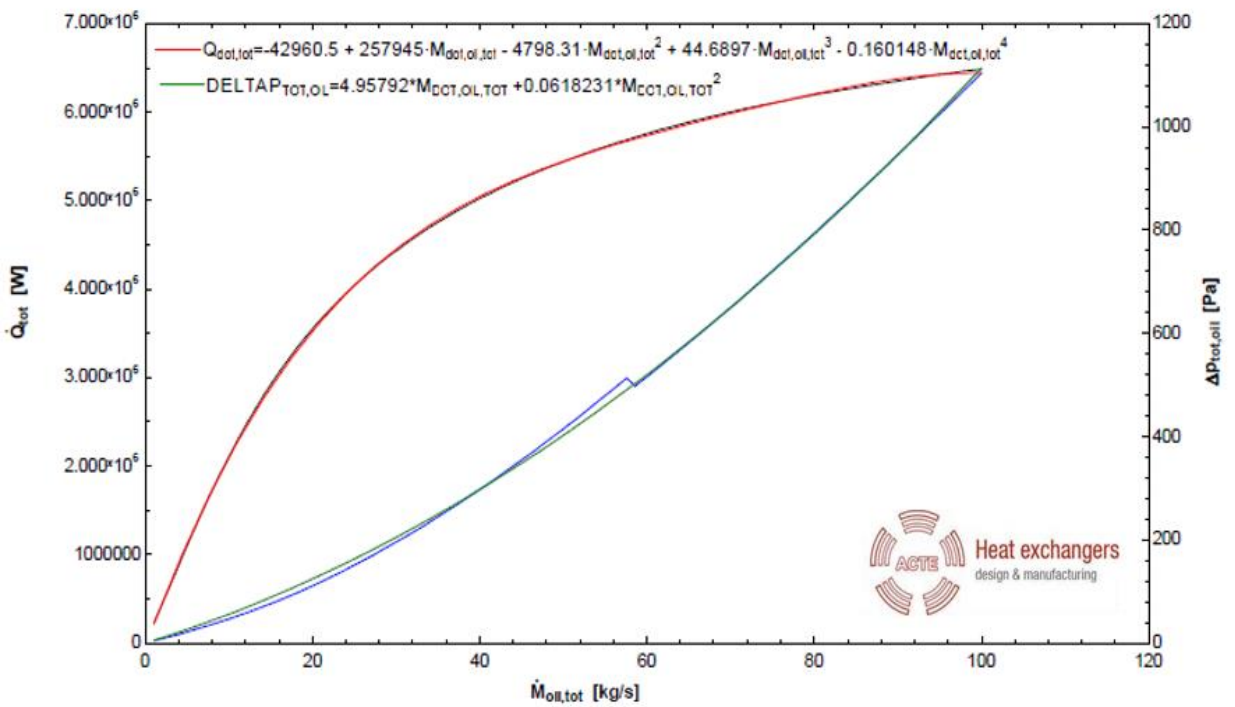


Figure 18. Heat transfer rate and pressure drop from the oil side of ACTE's recovery heat exchanger - case: turbo jet standard ducts [6].

For the other cases of turbofan and turbojet engines, enlarged ducts' layout, the same method was used. All the results are summarized hereunder [6]:

- turbofan engines – standard layout

$$AU_{oil} = 155671 + 17887,9 \cdot \dot{m}_{oil} - 304,779 \cdot \dot{m}_{oil}^2 + 3,31383 \cdot \dot{m}_{oil}^3 - 0,0133529 \cdot \dot{m}_{oil}^4$$

$$AU_g = 2640.84 + 266.145 \cdot \dot{m}_g - 0.292171 \cdot \dot{m}_g^2 + 0.000385631 \cdot \dot{m}_g^3 - 2.12264 \cdot 10^{-7} \cdot \dot{m}_g^4$$

$$\Delta P_{rhx} = 22.5786 \cdot \dot{m}_{oil} + 0.220964 \cdot \dot{m}_{oil}^2$$

- turbofan engines – enlarged layout

$$AU_{oil} = 183788 + 20655.4 \cdot \dot{m}_{oil} - 363.585 \cdot \dot{m}_{oil}^2 + 3.96338 \cdot \dot{m}_{oil}^3 - 0.01598 \cdot \dot{m}_{oil}^4$$

$$AU_g = 5050.66 + 330.141 \cdot \dot{m}_g - 0.224962 \cdot \dot{m}_g^2 + 0.000173883 \cdot \dot{m}_g^3 - 5.03499 \cdot 10^{-8} \cdot \dot{m}_g^4$$

$$\Delta P_{rhx} = 18.3751 \cdot \dot{m}_{oil} + 0.134763 \cdot \dot{m}_{oil}^2$$

- turbojet engines – standard layout

$$AU_{oil} = 151595 + 20312.6 \cdot \dot{m}_{oil} - 252.881 \cdot \dot{m}_{oil}^2 + 2.60173 \cdot \dot{m}_{oil}^3 - 0.0104334 \cdot \dot{m}_{oil}^4$$

$$AU_g = 26613.4 - 265.579 \cdot \dot{m}_g + 5.64536 \cdot \dot{m}_g^2 - 0.0194736 \cdot \dot{m}_g^3 + 0.0000214342 \cdot \dot{m}_g^4$$

$$\Delta P_{rhx} = 4.95792 \cdot \dot{m}_{oil} + 0.0618231 \cdot \dot{m}_{oil}^2$$

- turbojet engines – enlarged layout

$$AU_{oil} = 233224 + 27164.4 \cdot \dot{m}_{oil} - 402.038 \cdot \dot{m}_{oil}^2 + 4.38646 \cdot \dot{m}_{oil}^3 - 0.0178875 \cdot \dot{m}_{oil}^4$$

$$AU_g = 124855 - 928.157 \cdot \dot{m}_g + 8.67453 \cdot \dot{m}_g^2 - 0.0182398 \cdot \dot{m}_g^3 + 0.000012997 \cdot \dot{m}_g^4$$

$$\Delta P_{rhx} = 2.06245 \cdot \dot{m}_{oil} + 0.0269745 \cdot \dot{m}_{oil}^2$$

Regarding the finned tube heat exchanger, the thermal resistances from the gas and the oil sides and the pressure drop are taken from the same manufacturer data [6]:

- turbofan engines – standard layout

$$AU_{oil} = -1764.51 + 12809.4 \cdot \dot{m}_{oil} - 93.9784 \cdot \dot{m}_{oil}^2 + 0.911983 \cdot \dot{m}_{oil}^3 \\ - 0.00348018 \cdot \dot{m}_{oil}^4$$

$$AU_g = 2933.99 + 143.401 \cdot \dot{m}_g - 0.26855 \cdot \dot{m}_g^2 + 0.000729967 \cdot \dot{m}_g^3 \\ - 5.87837 \cdot 10^{-7} \cdot \dot{m}_g^4$$

$$\Delta P_{rhx} = 98.0052 \cdot \dot{m}_{oil} + 6.08598 \cdot \dot{m}_{oil}^2$$

- turbofan engines – enlarged layout

$$AU_{oil} = -2416.41 + 12591.9 \cdot \dot{m}_{oil} - 88.0962 \cdot \dot{m}_{oil}^2 + 0.845527 \cdot \dot{m}_{oil}^3 \\ - 0.00321197 \cdot \dot{m}_{oil}^4$$

$$AU_g = 3680.45 + 117.358 \cdot \dot{m}_g - 0.074087 \cdot \dot{m}_g^2 + 0.000227753 \cdot \dot{m}_g^3 \\ - 1.72810 \cdot 10^{-7} \cdot \dot{m}_g^4$$

$$\Delta P_{rhx} = 99.0154 \cdot \dot{m}_{oil} + 6.08287 \cdot \dot{m}_{oil}^2$$

- turbojet engines – standard layout

$$AU_{oil} = 12670,7 + 23519,8 \cdot \dot{m}_{oil} - 147,762 \cdot \dot{m}_{oil}^2 + 1.36134 \cdot \dot{m}_{oil}^3 \\ - 0.00503429 \cdot \dot{m}_{oil}^4$$

$$AU_g = -1025,87 + 370,737 \cdot \dot{m}_g - 2,04379 \cdot \dot{m}_g^2 + 0,00714481 \cdot \dot{m}_g^3 \\ - 0,00000952907 \cdot \dot{m}_g^4$$

$$\Delta P_{rhx} = 74,9242 \cdot \dot{m}_{oil} + 5,13906 \cdot \dot{m}_{oil}^2$$

- turbojet engines – enlarged layout

$$AU_{oil} = -19710 + 31732 \cdot \dot{m}_{oil} - 180.056 \cdot \dot{m}_{oil}^2 + 1.49489 \cdot \dot{m}_{oil}^3 \\ - 0.00510289 \cdot \dot{m}_{oil}^4$$

$$AU_g = -7233.6 + 3228.96 \cdot \dot{m}_g - 17.3767 \cdot \dot{m}_g^2 + 0.060352 \cdot \dot{m}_g^3 \\ - 0.0000802432 \cdot \dot{m}_g^4$$

$$\Delta P_{rhx} = 1.83472 \cdot \dot{m}_{oil} + 0.0962005 \cdot \dot{m}_{oil}^2$$

Since the exhaust gas mass flow rate for each case is known (see 2.3.1.1) and since the oil mass flow rate is an input of the model, the values of the thermal resistances from the gas and the oil sides of the recovery heat exchanger can be calculated using the polynomial laws. The value of the oil mass flow rate will be discussed in the following sections.

Using this information, an ε -NTU model of a single-phase heat exchanger has been implemented in order to develop a model of the recovery heat exchangers. The heat capacity rate of each stream is calculated as follows:

$$\dot{C}_g = \dot{m}_g \cdot C_{p_g} \quad (1)$$

$$\dot{C}_{oil} = \dot{m}_{oil} \cdot C_{p_{oil}} \quad (2)$$

Where:

- \dot{m}_g is the gas mass flow rate
- \dot{m}_{oil} is the oil mass flow rate
- $C_{p_g} = 1,05 [kJ/(kg \cdot K)]$ is the isobaric heat capacity
- $C_{p_{oil}} = 1,95 [kJ/(kg \cdot K)]$ is the isobaric heat capacity

The overall heat transfer coefficient AU_{rhx} has been calculated from the thermal resistance of each side of the recovery heat exchangers:

$$AU_{rhx} = \frac{1}{\frac{1}{AU_{oil}} + \frac{1}{AU_g}} \quad (3)$$

The effectiveness of the recovery heat exchanger has been calculated using the following expression for counter flow and for cross flow heat exchangers.

$$\varepsilon_{rhx} = \frac{1 - e^{(-NTU_{rhx} \cdot (1 - \omega_{rhx}))}}{1 - \omega_{rhx} \cdot e^{(-NTU_{rhx} \cdot (1 - \omega_{rhx}))}} \quad (4)$$

$$\varepsilon_{rhx} = 1 - e^{\left(\frac{e^{-NTU^{0,78} \cdot \omega_{rhx}} - 1}{NTU^{-0,22} \cdot \omega_{rhx}} \right)} \quad (5)$$

Where:

$$\omega_{rhx} = \frac{\dot{C}_{min,rhx}}{\dot{C}_{max,rhx}} \quad (6)$$

$$NTU_{rhx} = \frac{AU_{rhx}}{\dot{C}_{min,rhx}} \quad (7)$$

$$\dot{C}_{min,rhx} = \mathbf{Min} (\dot{C}_g ; \dot{C}_{oil}) \quad (8)$$

$$\dot{C}_{max,rhx} = \mathbf{Max} (\dot{C}_g ; \dot{C}_{oil}) \quad (9)$$

Considering the previous expressions and a heat balance across the recovery heat exchanger, the following equations have been established:

$$\dot{Q}_{rhx} = \dot{m}_g \cdot C_{pg} \cdot (T_{gsur_{rhx}} - T_{gex_{rhx}}) \quad (10)$$

$$\dot{Q}_{rhx} = \dot{m}_{oil} \cdot C_{p_{oil}} \cdot (T_{oil_{sur_{rhx}}} - T_{oil_{ex_{rhx}}}) \quad (11)$$

$$\dot{Q}_{rhx} = \varepsilon_{rhx} \cdot \dot{C}_{min,rhx} \cdot (T_{gsur_{rhx}} - T_{oil_{sur_{rhx}}}) \quad (12)$$

Where:

- \dot{Q}_{rhx} is the heat flow rate through the recovery heat exchanger
- $T_{gsu_{rhx}}$ is the gas temperature at the inlet of the recovery heat exchanger
- $T_{gex_{rhx}}$ is the gas temperature at the outlet of the recovery heat exchanger
- $T_{oil_{su_{rhx}}}$ is the oil temperature at the inlet of the recovery heat exchanger
- $T_{oil_{ex_{rhx}}}$ is the oil temperature at the outlet of the recovery heat exchanger

2.3.2 Oil loop

The main components of the oil loop are an oil pump, a pipe and the thermal oil. In this initial phase, some hypotheses about the secondary loop have been established. It has been assumed that the thermal oil is "Syltherm XLT" [7], the length of the pipe of the oil loop is 20 [m] and the internal diameter is 15 [cm].

Characteristics of the oil are considered constant:

- thermal oil density: $\rho_{oil} = 713 [kg/m^3]$
- thermal oil specific heat: $C_{p_{oil}} = 1,95 \left[\frac{kJ}{kg \cdot K} \right]$

2.3.2.1 Oil loop pressure drop

The pressure drop of the oil loop is composed by: the pressure drop that the thermal oil experiences when it flows through the recovery heat exchanger and the frictional pressure drops of the oil circuit.

$$\Delta P_{oil\ circuit} = \Delta P_{oil_{rhx}} + \Delta P_{oil_{friction}} \quad (13)$$

The pressure drops on the oil side of the recovery heat exchanger $\Delta P_{oil_{rhx}}$ have been calculated with the curves and the laws provided by ACTE company.

The frictional pressure drop is calculated assuming a friction factor $f_{factor,oil}$ of 0,02. Considering the known Darcy-Weisbach equation (14).

$$\Delta P_{oil\ friction} = f_{factor,oil} \cdot \rho_{oil} \cdot \frac{Length_{oil\ circuit}}{Diameter_{pipe_{oil\ circuit}}} \cdot \frac{c_{oil}^2}{2} \quad (14)$$

Where c_{oil} is the oil velocity and it is calculated as follows:

$$c_{oil} = \frac{\dot{m}_{oil}}{Area_{oil\ circuit} \cdot \rho_{oil}} \quad (15)$$

Where the cross section of the pipe is:

$$Area_{oil\ circuit} = \frac{\pi}{4} \cdot Diameter_{pipe_{oil\ circuit}}^2 \quad (16)$$

2.3.2.2 Oil pump model

The oil pump model is a very simple model that takes into account the required power to overcome the pressure drops of the oil circuit:

$$\dot{W}_{ideal_{oil\ pump}} = \dot{m}_{oil} \cdot \frac{\Delta P_{oil\ circuit}}{\rho_{oil}} \quad (17)$$

An overall efficiency for the oil pump $\varepsilon_{oil\ pump}$ has been set at 0,75:

$$\varepsilon_{oil\ pump} = \frac{\dot{W}_{ideal_{oil\ pump}}}{\dot{W}_{oil\ pump}} = 0,75 \quad (18)$$

In this way is possible to calculate the required power of the oil pump $\dot{W}_{oil\ pump}$.

2.3.3 Storage water tank

The hot water tank is a sensible heat storage with water as medium used to store/dissipate the heat produced by the recovery heat exchanger. The tank has been modelled by a one-node model with the water tank temperature T_{tank} as a state variable. It means that the stratification effects of the storage media were not taken into account. No ambient losses have been considered.

2.3.3.1 Storage water tank model

The storage tank has been modelled using a quasi-steady approximation. In this study the problem will be divided in time intervals. It has been considered that in each one of the time intervals, the conditions were steady. To approximate the unsteady nature of the system, the conditions of the problem change from an interval of time to the next one.

The temperature of the oil at the inlet of the water tank $T_{oil_{su_{tank}}}$ has been assumed equal to the temperature of the oil at the output of the recovery heat exchanger $T_{oil_{ex_{rhx}}}$. In the same way, the oil temperature at the output of the water tank $T_{oil_{ex_{tank}}}$ has been assumed equal to $T_{oil_{su_{rhx}}}$.

The initial temperature of the water contained in the tank is assumed 25[°C].

The recovered heat flow rate coming from the oil loop $\dot{Q}_{whr,tank}$ is expressed as:

$$\dot{Q}_{whr,tank} = \dot{m}_{oil} \cdot C_{p_{oil}} \cdot (T_{oil_{su_{tank}}} - T_{oil_{ex_{tank}}}) \quad (19)$$

The heat flow rate transferred from the water inside the tank to the water loop is expressed as $\dot{Q}_{tank,hx}$.

Furthermore, the efficiencies of both sides have been supposed constant. Their correlations with the heat flow rate transferred in the water tank were also written on EES. The values are shown in the table 2.

Table 2. Effectiveness of both sides of the water tank.

Location	Effectiveness [ϵ]
Oil side heat exchanger water tank	0,95
Water side heat exchanger water tank	0,80

The storage tank is modelled as follows:

$$\dot{Q}_{stored} = \dot{Q}_{whr,tank} - \dot{Q}_{tank,hx} \quad (20)$$

$$\dot{Q}_{stored} = \frac{dU}{d\tau} \quad (21)$$

Where U is the internal energy of the water tank, and $\dot{Q}_{tank,hx}$ is the heat transfer rate transferred either to the water loop system (boiler case) or to the evaporator (heat pump case).

Several configurations can be met:

- the engine test bench is running ($\dot{Q}_{whr,tank} > 0$) or is off ($\dot{Q}_{whr,tank} = 0$);
- there is a heating need ($\dot{Q}_{tank,hx} > 0$) or not ($\dot{Q}_{tank,hx} = 0$).

Additionally, the evolution of the internal energy of the storage can be expressed as:

$$\Delta U = \int_{\tau_1}^{\tau_2} \left(\frac{dU}{d\tau} \right) d\tau \quad (22)$$

Which allows to deduce the tank temperature T_{tank} at each time step, since the tank volume V_{tank} is an input of the model:

$$\Delta U = V_{tank} \cdot \rho_{water} \cdot C_{p,water} \cdot (T_{tank} - T_{tank_0}) \quad (23)$$

The value of the tank volume will be discussed in the following sections.

2.3.4 Water loop - boiler case

The water loop is composed of:

- a boiler
- a water pump
- a so-called “demand heat exchanger” that works between the water loop and the building water circuit

The boiler is fed with water coming from the heat exchanger placed inside the tank in the “boiler case”. The boiler efficiency has been assumed at 100%. The efficiency of the demand heat exchanger has been assumed at 90%.

The temperature of the water, coming from the water loop, at the inlet of the water tank $T_{wsu_{tank}}$ has been assumed equal to the temperature of the oil loop water at the output of the demand heat exchanger $T_{wex_{hx}}$. The temperature of the oil loop water at the inlet of the demand heat exchanger $T_{wsu_{hx}}$ has been assumed:

$$T_{wsu_{hx}} [^{\circ}C] = T_{to_{demand}} [^{\circ}C] + 5 [^{\circ}C] \quad (24)$$

Where $T_{to_{demand}}$ is the water temperature of the buildings heating circuit at the outlet of the demand heat exchanger.

Like for the other components, all the balances at the boiler and at the demand heat exchanger have been written on EES program.

2.3.5 Heating circuit

The temperature regime for the water heating circuit has been considered in the present study as follows:

$$T_{from_{demand}} = 45 [^{\circ}C] \quad (25)$$

$$T_{to_{demand}} = 60 [^{\circ}C] \quad (26)$$

Where $T_{from\,demand}$ is the water temperature of the buildings heating circuit at the inlet of the demand heat exchanger.

2.3.6 Heat pump

It has been chosen to use the “Consoclim model” [8]. This model allows to predict the behavior of cooler or heat pump via three polynomial laws. This involves the identification of parameters via constructor data. Two of these laws, *EIRFT* and *CAPFT*, allow to calculate the COP and the heating capacity at full load according to two variables:

- The evaporator temperature T_{ev}
- The water exhaust condenser temperature T_w

The last law *EIRFPLR* is used to compute partial load performance.

These laws are given hereunder:

$$EIRFT = \frac{COP_{nom}}{COP_{fl}} = C_0 + C_1 \cdot \Delta T + C_2 \cdot \Delta T^2 \quad (27)$$

$$\Delta T = \frac{T_{ev}}{T_w} - \left(\frac{T_{ev}}{T_w} \right)_{nom} \quad (28)$$

$$CAPFT = \frac{\dot{Q}_{fl}}{\dot{Q}_{nom}} = D_0 + D_1 \cdot (T_{ev} - T_{ev,nom}) + D_2 \cdot (T_w - T_{w,nom}) \quad (29)$$

$$EIRFPLR = \frac{\dot{W}_{pl}}{\dot{W}_{fl}} = K_1 + (K_2 - K_1) \cdot PLR + (1 - K_2) \cdot PLR^2 \quad (30)$$

$$PLR = \frac{\dot{Q}_{pl}}{\dot{Q}_{fl}} \quad (31)$$

$$COP_{fl} = \frac{\dot{Q}_{fl}}{\dot{W}_{fl}} \quad (32)$$

$$COP_{pl} = \frac{\dot{Q}_{pl}}{\dot{W}_{pl}} \quad (33)$$

Where:

- The indexes "*fl*" and "*pl*" respectively indicate the partial load operation and the full load operation;
- The nominal index "*nom*" is used to quantify the values when the heat pump is working under nominal conditions (i.e. 10°C for inlet evaporator temperature and 35°C for outlet water temperature);
- \dot{Q} represents the thermal power supplied to the condenser and \dot{W} the electric power consumed by the compressor.

The heat pump operates at variable speed up down to 30% of Part Load Ratio (PLR). The catalog data stops for a partial load of 30%. Below this value, the heat pump operates in ON / OFF mode. Information on the behavior of the heat pump operating on ON / OFF could not be obtained, even from the manufacturer.

In order to take into account the degradation related to ON / OFF operation for partial loads of less than 30%, a polynomial stemming from P. Rivière's thesis was used [9]. The latter proposes a variation of COP with respect to the COP at full load, for compressors operating only in ON / OFF:

$$\frac{COP_{pl}}{COP_{fl}} = \frac{PLR}{a \cdot PLR + b} \quad (34)$$

In the case of a heat pump equipped with a variable speed compressor, for PLR lower than 30%, the ON/OFF mode is activated with an ON mode corresponding to a PLR of 30%. In order to take this fact into account, the previous equation thus becomes:

$$\frac{COP}{COP_{30\%}} = \frac{PLR_{ON/OFF}}{a \cdot PLR_{ON/OFF} + b} \quad (35)$$

And $PLR_{ON/OFF}$ is defined by:

$$PLR_{ON/OFF} = \frac{PLR}{0.3} \quad (36)$$

By default, it has been used for parameters a and b, the parameters proposed by P. Rivière (2004):

- $a = 0.77$;
- $b = 0.229$.

Parameters used in the frame of the present work correspond to the average values based on a market survey realized in the frame of the “FlexiPAC” project [10]:

Table 3. Heat pump parameters.

T_{evnom}	T_{wnom}	COP_{nom}	C_0	C_1	C_2	D_0	D_1	D_2	K_1	K_2	a	b
10	35	4.02	1.033	-8.31	37.88	1.008	0.028	-0.005	0	0.64	0.77	0.229

Another parameter that is fixed is \dot{Q}_{nom} . A parametric study of \dot{Q}_{nom} , in order to minimize the payback time, will be developed in the following sections.

2.4 Test bench general assumptions for Zaventem site

The tests period lasts from January until March and from September until December.

It is also assumed the first of January as a Monday, in order to well organize the whole year:

- $1 \text{ year} = 365 \text{ day}$
- $1 \text{ year} = 365 \cdot 24 = 8760 \text{ h}$

There are 5 hours of test per day and they go from 8am to 1pm. The tests are carried out only during working days, from Monday to Friday.

2.4.1 ON-OFF boiler period

The existing boiler is used to heat buildings near the test bench.

The boiler works:

- from October to April,
- considering five working days per week,
- for 10 hours per day (from 8 am to 6 pm).

It is off:

- from May to September,
- during the weekend.

2.4.2 Boiler demand

The boiler demand, as mentioned before, is 40000 liters per year. In order to calculate the monthly demand, the Heating degree day (HDD) method has been used [11]. HDD is a measurement designed to quantify the demand for energy needed to heat a building. HDD is derived from measurements of outside air temperature. The heating requirements for a given building at a specific location are considered to be directly proportional to the number of HDD at that location. Zaventem’s test bench is located in Brussels airport area. The HDD monthly schedule for Brussels is:

Table 4. HDD per months in Brussels [11].

J	F	M	A	M	J	J	A	S	O	N	D	TOTAL
365,8	330,6	254,2	159	61	15,2	0	0	22,5	114,7	246	344	1913

The formula used to calculate the monthly demand [11] is:

$$\begin{aligned}
 & \text{Monthly demand} \\
 & = 40000 \left[\frac{l}{\text{year}} \right] \\
 & \cdot \left(\frac{\text{HDD value of the month considered}}{\text{HDD total value} - \sum \text{HDD values of the months when the boiler is off}} \right)
 \end{aligned}
 \tag{37}$$

The results are:

Table 5. Consumed fuel per month in Zaventem site

Month	<i>l</i>
January	8066,15
February	7289,97
March	5605,29
April	3506,06
October	2529,22
November	5424,48
December	7587,65

The working days per month are:

Table 6. Working days per month in Zaventem site.

Month	Days
January	23
February	20
March	22
April	21
October	23
November	22
December	22

Then, the daily and hourly demand has been calculated as detailed below:

$$\text{Daily demand} = \frac{\text{Monthly demand}}{\text{Working days}} \quad (38)$$

$$\text{Hourly demand} = \frac{\text{Daily demand}}{10} \quad (39)$$

Where 10 represents the number of working hours per day.

The demand was also converted in kWh, according to the type of used fuel which is oil fuel [12]:

$$1[l] = 12,2 [kWh] \quad (40)$$

Table 7 shows the fuel consumption.

Table 7. Fuel consumption in Zaventem site

Month	<i>l</i>	Working days	<i>l</i>/Day	Working hours/Day	<i>l</i> /Working hours	kWh/ Working hours
January	8066,15	23	350,70	10	35,07	427,86
February	7289,97	20	364,50	10	36,45	444,69
March	5605,29	22	254,79	10	25,48	310,84
April	3506,06	21	166,96	10	16,70	203,69
October	2529,22	23	109,97	10	11,00	134,16
November	5424,48	22	246,57	10	24,66	300,81
December	7587,65	22	505,84	10	50,58	440,80

In the example below is shown a typical working and testing day of January:

Table 8. Consumed fuel per hour in Zaventem site for a typical January day.

Time [h]	Boiler Demand [l]	Boiler Demand [kWh]	Test Engine (ON/OFF)
1	0	0	0
2	0	0	0
3	0	0	0
4	0	0	0
5	0	0	0
6	0	0	0
7	0	0	0
8	0	0	0
9	35,07	427,86	1
10	35,07	427,86	1
11	35,07	427,86	1
12	35,07	427,86	1
13	35,07	427,86	1
14	35,07	427,86	0
15	35,07	427,86	0
16	35,07	427,86	0
17	35,07	427,86	0
18	35,07	427,86	0
19	0	0	0
20	0	0	0
21	0	0	0
22	0	0	0
23	0	0	0
24	0	0	0

In table 7 the third column shows when the test bench is running:

- 1 = the test bench is on,
- 0 = the test bench is off.

2.5 Test bench general assumptions for Rygge site

Twenty-nine motors were tested during 2016 (110,000 liters of fuel consumed). A test duration is comprised between 4 and 6 hours. The tests were distributed over 11 months because the base is indeed closed during the month of July.

For our simulation, a mean average duration of 5 hours per test is considered. It is also assumed the first of January as a Monday, in order to well organize the whole year:

- 1 year = 365 day
- 1 year = 365 · 24 = 8760 h

The 5 hours of test per day go from 8am to 1pm. It has been assumed that the tests are performed only on Monday. The 29 tests are distributed over the year as shown in table 9:

Table 9. Number of engines tested per month.

	Month											
	J	F	M	A	M	J	J	A	S	O	N	D
Number of tested engines	3	2	3	2	3	2	0	3	2	3	3	3

2.5.1 ON-OFF boiler period

The existing boiler is used to heat the main building, which is composed by the test bench and the preparation room, and a neighbouring storage building.

The boiler is supposed to work the whole year since it is also used to maintain a minimum temperature of 8°C in the neighbouring storage building (Hush House storage).

However, concerning the boiler use for the main building, the test bench and the preparation room, the following assumptions have been used.

The boiler is ON:

- from October to May,
- considering five working days per week,
- for 10 hours per day (from 8 am to 6 pm).

It is OFF:

- from June to September,
- during the weekend.

2.5.2 Boiler demand

The LPG (propane) boiler consumed about 10000 [kg] during the year for the test bench and the preparation room. The same boiler was also used to heat the neighbouring storage building at 8[°C] during cold periods. So, 5000 additional [kg] were consumed over the year to perform this task. In total, the LPG consumption is 15000 [kg] per year for the test bench, the preparation room and the neighbouring storage building.

In order to calculate the monthly demand for the test bench and the preparation room, the Heating Degree Day (HDD) method has been used [11]. Rygge’s test bench is located in Norway. The HDD monthly schedule for Rygge is:

Table 10. HDD per months in Rygge [11].

J	F	M	A	M	J	J	A	S	O	N	D	TOTAL
413	418	484	463	397	307	145	49	22	34	101	233	3066

Considering the same number of working days per month and the same number of working hours per day of Zaventem site, the total amount of fuel per working hour depending on

the month is given in table 11. The demand is also converted in [kWh], according to the type of fuel, LPG in this case [13]:

$$1[\text{kg}] = 13,7 [\text{kWh}] \quad (41)$$

Table 11. Fuel consumption in Rygge for the test bench and the preparation room.

Month	kg	Working days	kg/Day	Working hours/Day	kg/Working hours	kWh/Working hours
January	1624,07	23	70,61	10	7,06	96,74
February	1643,73	20	82,19	10	8,22	112,60
March	1903,26	22	86,51	10	8,65	118,52
April	1820,68	21	86,70	10	8,67	118,78
May	1561,15	23	67,88	10	6,79	92,99
October	133,70	23	5,81	10	0,58	7,96
November	397,17	22	18,05	10	1,81	24,73
December	916,24	22	61,08	10	6,11	83,68

Concerning the boiler demand for the neighbouring storage building, the same methodology than the Heating Degree Day has been applied, except that the base temperature for the HDD determination is now chosen to 8°C [11]. The boiler has been supposed to work all year long to maintain the minimum temperature and the heating requirements is directly proportional to the number of HDD calculated with a base temperature equal to 8°C. The total amount of consumed fuel for maintaining this temperature is equal to 5000 kg of propane per year.

In the example below is shown a typical working and testing day of January.

Table 12. Consumed fuel per hour in Rygge site for a typical January day.

Time [h]	Boiler Demand [kg]	Boiler Demand [kWh]	Boiler Demand storage building [kg]	Boiler Demand storage building [kWh]	Boiler Demand TOT [kg]	Boiler Demand TOT [kWh]	Test Engine (ON/OFF)
1	0	0	1,51	20,71	1,51	20,71	0
2	0	0	0,96	13,13	0,96	13,13	0
3	0	0	0,43	5,87	0,43	5,87	0
4	0	0	0,47	6,40	0,47	6,40	0
5	0	0	0,51	6,94	0,51	6,94	0
6	0	0	0,55	7,47	0,55	7,47	0
7	0	0	0,58	8,01	0,58	8,01	0
8	0	0	0,62	8,54	0,62	8,54	0
9	7,06	96,74	0,66	9,07	7,72	105,81	1
10	7,06	96,74	0,70	9,61	7,76	106,34	1
11	7,06	96,74	0,72	9,82	7,78	106,56	1
12	7,06	96,74	0,69	9,39	7,75	106,13	1
13	7,06	96,74	0,65	8,97	7,72	105,70	1
14	7,06	96,74	0,65	8,86	7,71	105,60	0
15	7,06	96,74	0,63	8,65	7,69	105,38	0
16	7,06	96,74	0,63	8,65	7,69	105,38	0
17	7,06	96,74	0,64	8,75	7,70	105,49	0
18	7,06	96,74	0,65	8,86	7,71	105,60	0
19	0	0	0,66	9,07	0,66	9,07	0
20	0	0	0,68	9,29	0,68	9,29	0
21	0	0	0,69	9,50	0,69	9,50	0
22	0	0	0,71	9,71	0,71	9,71	0
23	0	0	0,72	9,93	0,72	9,93	0
24	0	0	0,74	10,14	0,74	10,14	0

2.6 Economic aspects

The total cost of the solution is estimated as the sum of the single components cost:

1. Recovery heat exchanger cost
2. Oil loop cost

3. Storage system cost
4. Boiler and water loop cost
5. Heat pump cost
6. Maintenance cost

Energy prices and the payback time calculation are also discussed in the present section.

2.6.1 Recovery heat exchanger cost

The price of the recovery heat exchangers has been provided by ACTE. For the finned tube recovery heat exchangers, prices came from the same manufacturer data [6]. Both of them are based on the conditions of the different types of test benches.

Table 13. Cost of the recovery heat exchangers [6].

Cost of the RHX [€]			
Test bench	Type of duct	RHX ACTE	RHX finned tube
T. Fan	Standard	59700	36400
	Enlarged	73700	36400
T. Jet	Standard	87300	38600
	Enlarged	114100	227300

2.6.2 Oil loop cost

The main components of the oil loop are:

- Thermal oil (Syltherm 800)
- Oil pump
- Pipes.

The amount of thermal oil that has been considered is the one to completely fill the oil loop pipes. The cost of the thermal oil is 30 [€/kg] [7]. The price of the steel pipes has been estimated with the help of suppliers as well as the oil pump.

The table 14 shows a resume of the oil loop cost.

Table 14. Cost of the oil loop.

Oil loop cost [€]				
Item	Specification	Quantity	Unit of measurement	Cost
Thermal oil	Syltherm 800	252	[kg]	7600
Pump	-	1	/	3000
Pipes	15 cm diameter - steel	20	[m]	500
Total cost [€]				
				11100

2.6.3 Storage system cost

According to some data, a storage system cost varies between 150 and 250 € per m^3 [14].

It has been assumed an average cost of 200 € per m^3 for our simulations.

2.6.4 Boiler and water loop cost

Since the boiler was supposed to be present in the considered test centers, its cost has not been considered as part of the total investment cost of each solution. Also the water loop, which includes the water pump and the demand heat exchanger, was supposed to be present, so its cost has not been considered.

2.6.5 Heat pump cost

For the estimation of the heat pump cost, a cost of 400 [€/kWh] is considered. The heat pump cost, is based on data of heat pump manufacturers [15].

2.6.6 Maintenance cost

No maintenance cost has been considered in this study.

2.6.7 Energy prices

Prices considered in this study have been summarized in the table 15:

Table 15. Energy prices [16] [17] [18].

	Belgium	Norway
Electricity [€/kWh]	0.11	0.08
LPG[€/l] => [€/kWh]	-	0.629 => 0.09
Fuel oil [€/l] => [€/kWh]	0.6 => 0.05	-

2.7 Discussion of the results

Numerical results are discussed in this section for both investigated solutions.

2.7.1 Boiler solution for Zaventem site

A parametric study has been developed for each solution in order to determine what are the oil mass flow rate and the storage tank volume that minimise the PBT. This will be discussed in the next paragraph.

Figure 19 represents the heat transfer rates evolution during one day for turbofan standard test bench with ACTE's heat exchanger, an oil mass flow rate of $40 \left[\frac{\text{kg}}{\text{s}} \right]$ and a storage tank volume of $50 \left[\text{m}^3 \right]$. As it can be observed, the demand (\dot{Q}_{demand}), remains constant during the ten working hours as previous seen in the section of the boiler demand for Zaventem site. If the waste heat recovery was not performed, the boiler (\dot{Q}_{boiler}) would have provided the same exact heat transfer rate than the one required (\dot{Q}_{demand}). The green line ($\dot{Q}_{whr,tank}$) represents the heat transfer rate recovered and transmitted by means of the oil loop to the storage water tank. As it can be observed, the heat transfer rate ($\dot{Q}_{whr,tank}$) is always equal to zero except when the engine is running. Furthermore, it decreases because, meanwhile the tests are running, the tank temperature increases. The red line (\dot{Q}_{stored}) is defined as the difference between the heat transfer rate recovered by means of the oil loop and the one transferred to the water loop ($\dot{Q}_{stored} = \dot{Q}_{whr,tank} - \dot{Q}_{tank}$) and it represents the power stored in the water tank. During the 5 hours of engine tests, the power stored in the water tank (\dot{Q}_{stored}) is superior to zero because the heat transfer rate recovered and transmitted to the storage tank ($\dot{Q}_{whr,tank}$, green line) is higher than the one transferred to the water loop (\dot{Q}_{tank} , blue line) to preheat the water for the boiler. Obviously, the sum of \dot{Q}_{boiler} and \dot{Q}_{tank} is equal to \dot{Q}_{demand} . Energy savings can be deduced from the area comprised between the purple and the black lines.

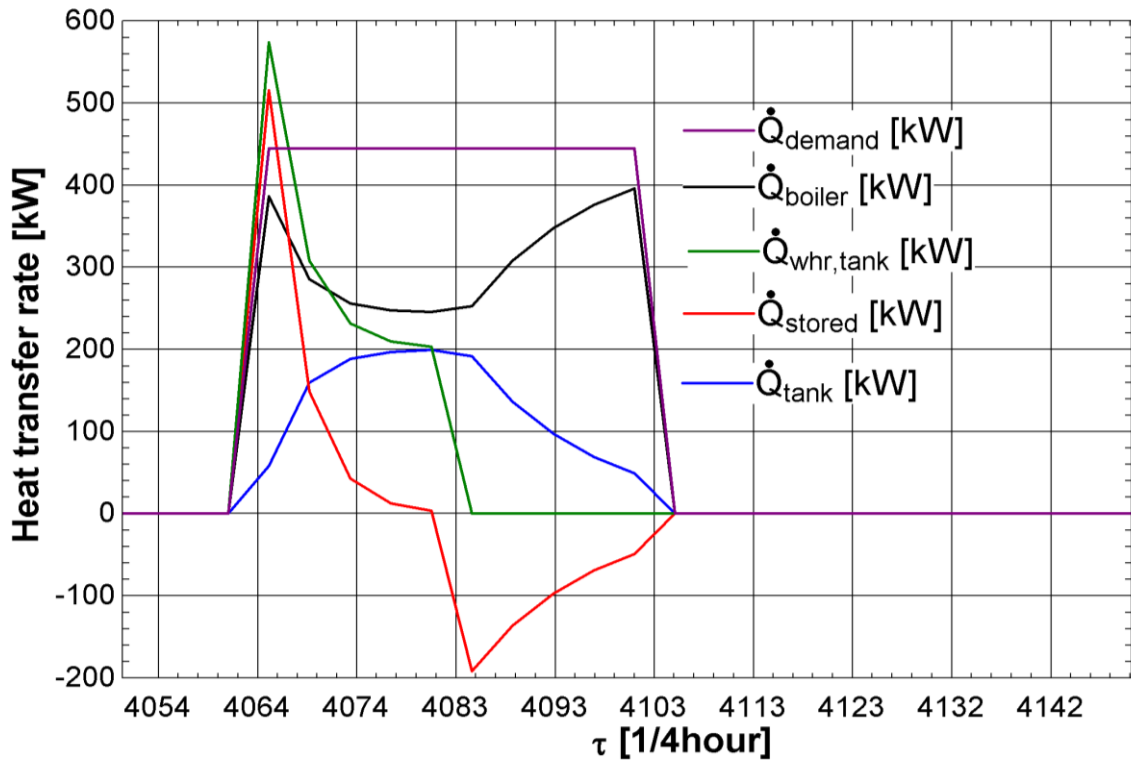


Figure 19. Heat transfer rates evolution during a day - turbo fan standard case with an ACTE recuperator, an oil mass flow rate of 40 [kg/s] and a storage tank volume of 50[m³].

Figure 20 represents the water tank temperature evolution for a typical week of January. The peaks correspond to the tests of engine, which raised the temperature inside the tank. Then, heat is transferred to the water while engine tests are off and the temperature drops.

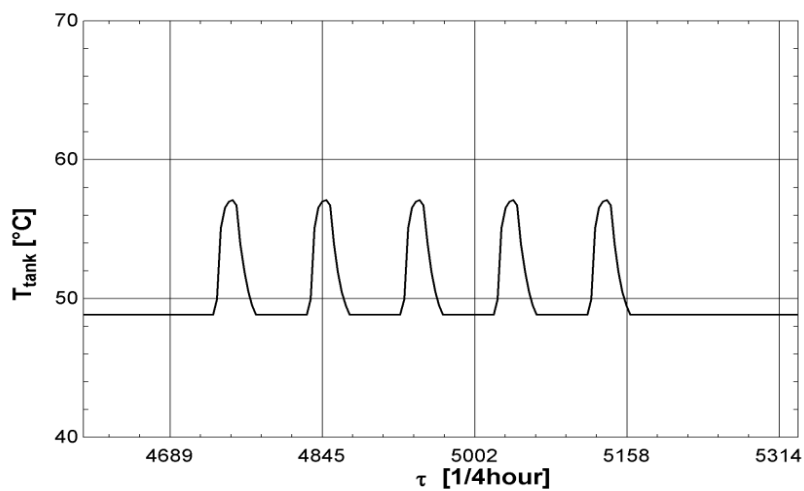


Figure 20. Tank temperature evolution during a week of February.

It can be also observed that the temperature inside the tank is limited to around 57°C due to the exhaust gas temperature (turbofan exhaust gas conditions).

2.7.2 Boiler solution for Rygge site

Concerning the Rygge site and as shown in figure 21, it has been decided to stop the heat recovery once the tank temperature was above the 100°C in order to keep the water in a liquid phase.

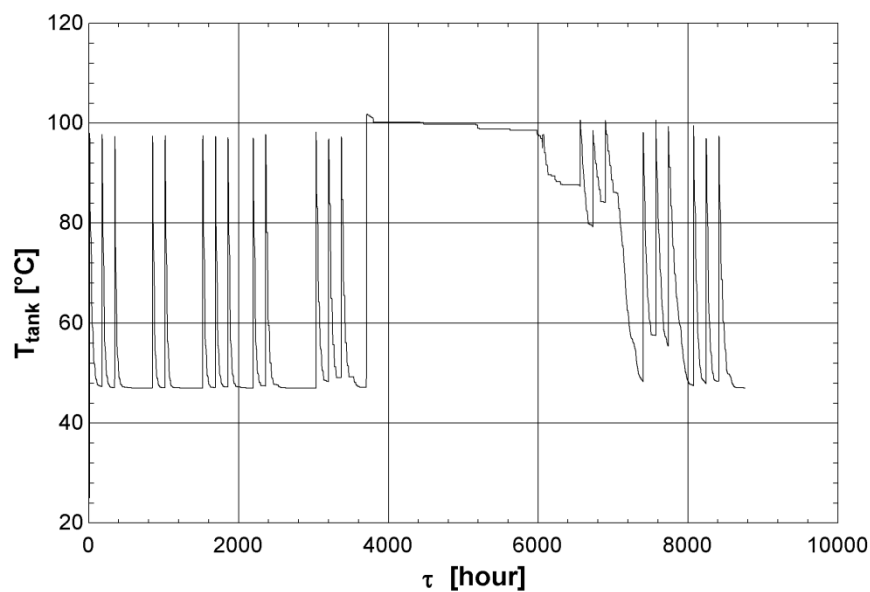


Figure 21. Tank temperature evolution yearly basis.

Figure 22 shows the evolution of the heat flow rates already presented in the previous section for one particular case. The main difference between Zaventem and Rygge site is that there is a huge amount of recovered heat transfer rate at the beginning of each engine tests (one per week - assumed to be on Monday morning for two or three days per month). This is due to a higher exhaust gas temperature from the tested engine (turbojet compared to turbofan). So, at the beginning of the week, there is a huge amount of heat transfer rate recovered in a really small amount of time (the time to reach 100°C in the tank). This amount of energy is highly dependent on the storage tank volume since there is a limitation

of 100°C inside the tank. This power is first stored in the storage tank and then released during the whole week. Thus, during the first and the second day of the two weeks considered in the example of figure 22, the boiler is not running since there is enough heat stored in the tank. Then, the boiler has to be turned on to provide the heating need, and the same situation as described in the previous section is encountered. Furthermore, it is possible to see that for this site the demand is not steady because of the storage building that needs to be heat during the whole year, every day.

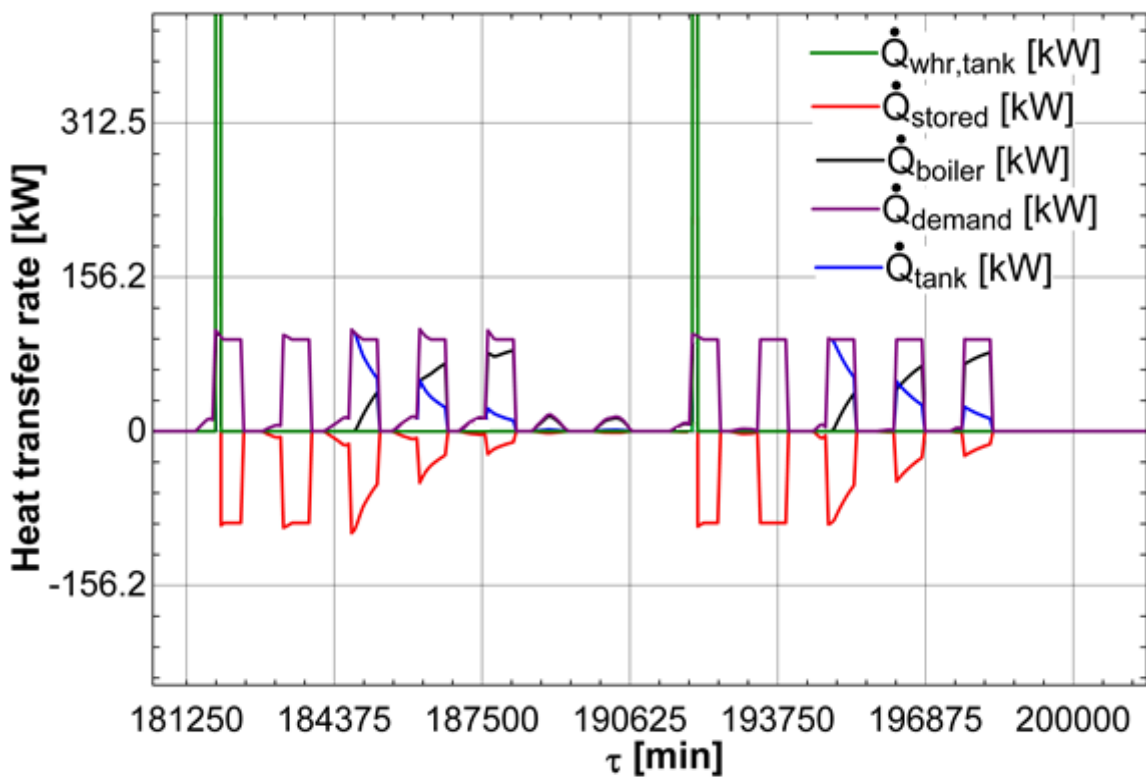


Figure 22. Heat transfer rates evolution during two weeks - turbo jet standard case with an ACTE recuperator, an oil mass flow rate of 40 [kg/s] and a storage tank volume of 60 [m³].

2.7.3 Heat pump solution for Zaventem site

Concerning the heat pump solution, there are three parameters that can result in an optimization: the oil mass flow rate, the nominal thermal power supplied to the condenser and the storage tank volume.

Figure 23 represents the heat transfer rates evolution during one week of February for a particular case (see legend of the figure). As it can be observed, the demand remains constant during the ten working hours. If the waste heat recovery was not performed, the boiler (\dot{Q}_{boiler}) would have provided the same exact heat transfer rate than the one required (\dot{Q}_{demand}). The green line ($\dot{Q}_{whr,tank}$) represents the heat transfer rate recovered and transmitted by means of the oil loop to the storage water tank. As it can be observed, the heat transfer rate is always equal to zero except when the engine is running. The red line (\dot{Q}_{stored}) is defined in the previous section and represents the power stored in the tank. During the 5 hours of engine tests, \dot{Q}_{stored} is superior to zero because the heat flow rate recovered and transmitted to the storage tank is higher than the heat flow rate transferred to the heat pump evaporator. The heat flow rate transferred at the condenser of the heat pump is expressed as \dot{Q}_{cd} . If the heat pump is not powerful enough to provide the heating need ($\dot{Q}_{cd} < \dot{Q}_{demand}$), then the backup boiler is turned on. Obviously, the sum of \dot{Q}_{boiler} and \dot{Q}_{cd} is equal to \dot{Q}_{demand} .

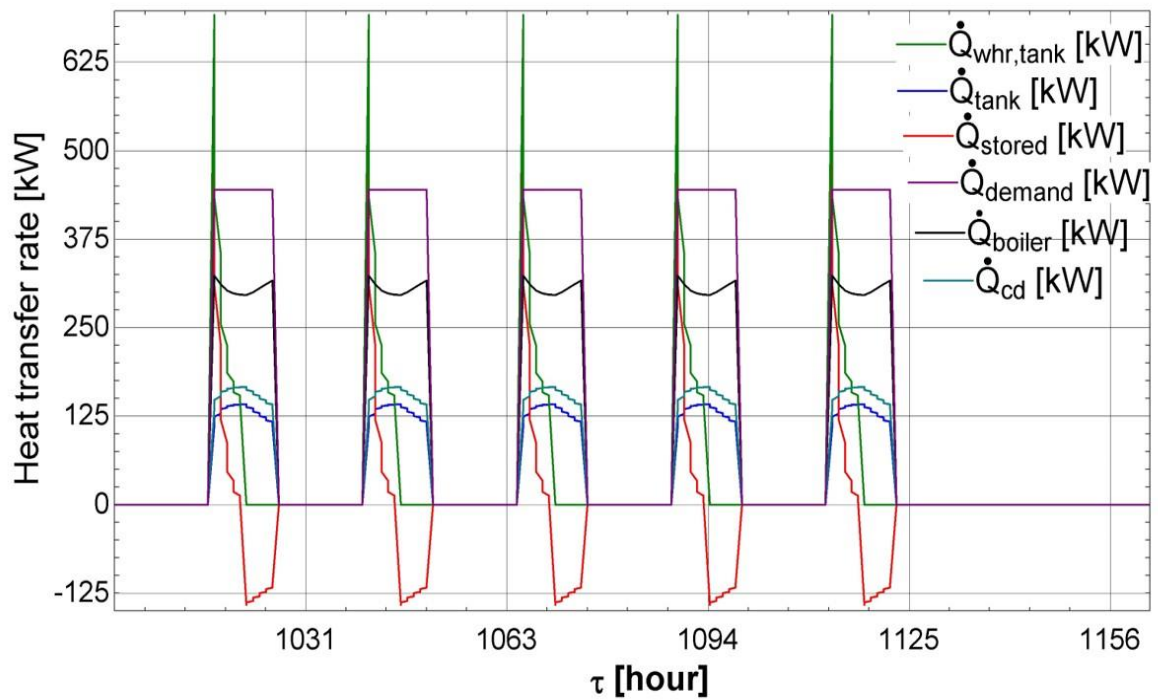


Figure 23. Heat transfer rates evolution during a week - turbo fan standard case with an ACTE recuperator, an oil mass flow rate of 40[kg/s], a storage tank volume of 50[m³] and a $\dot{Q}_{cd_{nom}}$ of 100 [kW].

Figure 24 shows the temperature evolution inside the tank and the related COP. The five peaks on the right side of the figure represent one week.

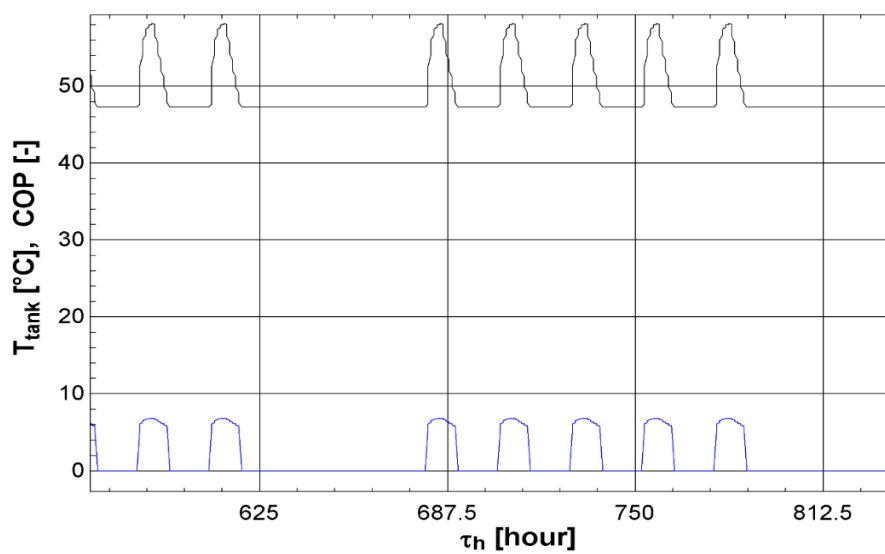


Figure 24. Tank temperature and COP estimation.

2.7.4 Heat pump solution for Rygge site

In the section dedicated to the boiler solution for Rygge site, it has been possible to evaluate the water tank temperature, which is most of the time higher than the one of the water required by the building circuit. So, the heat pump system doesn't represent a feasible solution for Rygge.

2.8 Payback time

One of the most important criteria to evaluate the GO/ NO GO decision of the implementation of a waste heat recovery system in the test benches is the payback time. The payback time is calculated using the results of the previous sections and it is evaluated for all the different cases. It is assumed that the test benches work always at full load.

The payback time is calculated as follow:

$$PBT = \frac{\text{Total Investment Cost [€]}}{\text{Savings } \left[\frac{\text{€}}{\text{year}} \right]} \quad (42)$$

The savings per year is calculated as the current expense for the heating needs minus the expense related to investigated solution with heat recovery.

A parametric study has been developed for each solution in order to minimise the PBT.

2.8.1 Boiler solution

Concerning the boiler solution, there are two parameters that can result in an optimization:

- the oil mass flow rate,
- the storage tank volume.

In the following figure 25 is possible to see an example of the parametric study results for Zaventem site (turbofan engines) with a standard layout and an ACTE heat exchanger. The

mass flow rate \dot{m}_{oil} is expressed in $\left[\frac{kg}{s}\right]$, the tank volume V_{tank} in $[m^3]$ and the payback time in $[year]$.

1..29	\dot{m}_{oil}	V_{tank}	PBT
Run 1	10	5	18.16
Run 2	10	10	17.67
Run 3	10	20	16.99
Run 4	10	30	16.66
Run 5	10	40	16.56
Run 6	10	50	16.64
Run 7	20	10	13.76
Run 8	20	20	13.05
Run 9	20	30	12.65
Run 10	20	40	12.46
Run 11	20	50	12.41
Run 12	30	10	12.63
Run 13	30	20	11.91
Run 14	30	30	11.49
Run 15	30	40	11.28
Run 16	30	50	11.19
Run 17	30	60	11.2
Run 18	40	10	12.08
Run 19	40	20	11.36
Run 20	40	30	10.94
Run 21	40	40	10.71
Run 22	40	50	10.62
Run 23	40	60	10.61
Run 24	50	10	11.49
Run 25	50	20	11.04
Run 26	50	30	10.61
Run 27	50	40	10.39
Run 28	50	50	10.29
Run 29	50	60	10.27

Figure 25. Payback time parametric study for Zaventem site – turbofan standard with an ACTE recuperator.

The results of the minimum payback time for Zaventem other cases are shown in table 16.

Table 16. Minimum payback times for the boiler solution in Zaventem site.

ZAVENTEM				
Type of ducts layout	Type of heat exchanger	\dot{m}_{oil} [kg/s]	V_{tank} [m ³]	PBT [Years]
Standard	Finned tube	50	40	7,8
Enlarged	GAP (ACTE)	50	60	20,1
Enlarged	Finned tube	50	40	13,3

Table 16 shows the results of the payback time optimization while varying the oil flow rate and the storage tank size for Zaventem site. As shown, the estimated pay back times are relatively high (minimum value is equal to 7,8 years) compared to the ones considered acceptable generally by the companies. Those results can be explained:

- by a limitation in terms of the temperature that the tank can achieved, the theoretical maximal value is equal to the low exhaust gas temperature,
- by a cost of the heat exchanger and the other parts of the system quite high,
- by too low engine test hours compared to the building heating need.

The results for Rygge site are shown in table 17.

Table 17. Minimum payback times for the boiler solution in Rygge site

RYGGE				
Type of ducts layout	Type of heat exchanger	\dot{m}_{oil} [kg/s]	V_{tank} [m ³]	PBT [Years]
Standard	GAP (ACTE)	50	60	9,28
Standard	Finned tube	40	50	5,3
Enlarged	GAP (ACTE)	40	60	11,5
Enlarged	Finned tube	40	50	22,2

Table 17 shows the results of the payback time optimization while varying the oil flow rate and the storage tank size for Rygge site. Once again, it can be observed that the PBT is relatively high. This can be explained by the limitation of the tank temperature at 100°C, a cost of the investment quite high, too low engine test hours compared to the building heating need. In order to recover more energy, higher storage tank volumes could be considered but it would raise the investment cost and brings to a technically unfeasible solution.

2.8.2 Heat pump solution for Zaventem site

Concerning the heat pump solution, there are three parameters that can results in an optimization:

- the oil mass flow rate,
- the nominal thermal power supplied to the condenser,
- the storage tank volume.

In the following table 18 is possible to see the results of the minimum payback times for all the cases.

Table 18. Minimum payback times for the heat pump solution in Zaventem site.

ZAVENTEM					
Type of ducts layout	Type of heat exchanger	$\dot{Q}_{cd, nom}$ [kW]	\dot{m}_{oil} [kg/s]	V_{tank} [m ³]	PBT [Years]
Standard	GAP (ACTE)	100	50	50	23,7
Standard	Finned tube	100	40	30	11,5
Enlarged	GAP (ACTE)	100	50	40	22,1
Enlarged	Finned tube	100	40	40	13,8

Table 18 shows the results of the payback time optimization changing the oil flow rate, the storage tank size and the nominal thermal power supplied to the condenser for Zaventem site. The estimated pay back times are relatively high (minimum value is equal to 11,5

years). The heat pump solution payback time is strongly related to the difference between the fuel and the electricity price, as primary sources.

As in the boiler solution, the results depend on too low engine test hours compared to the building heating need.

Furthermore, the price of the heat pump represents an investment additional cost.

Looking at the PBT results this solution has to be considered unfeasible for Zaventem test bench.

3 Experimental investigation

In this section, the experimental one, a new ACTE's type of recovery heat exchanger, which could be used to recover energy from the hot exhaust gas, is tested in order to verify its performances.

The tests on the heat exchanger have been performed on the test bench assembled at the Thermodynamics Laboratory of the University of Liège.

3.1 Heat exchanger description

The heat exchanger that has been tested in this part of the study is produced by ACTE company. The model of ACTE's heat exchanger is: GAP 50-3-3 . It is a counter flow heat exchanger.

In the GAP heat exchanger, the heat exchange surface and external volume are optimised. The GAP waste heat recuperator has been designed to answer heat recovery needs for applications that require highly effective exchange within a small volume and it has been specially designed to fit within chimney ducts. ACTE GAP technology has been developed to recover heat from the hot waste gas released during existing industrial processes without impacting the process itself.

The annular shape enables an ideal integration of the heat exchanger into all asymmetric installations as chimney ducts. An example can be seen in figure 26.

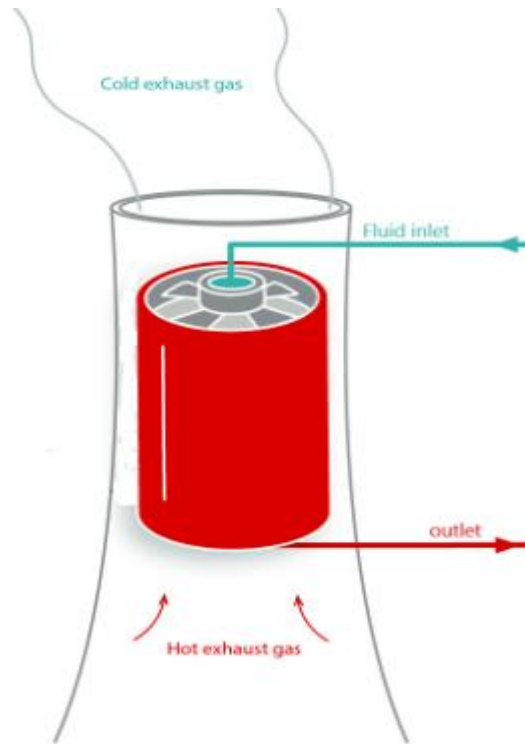


Figure 26. Installation of the ACTE's GAP heat exchanger in a chimney [19].

Figure 27 shows a picture of the GAP heat exchanger [19].



Figure 27. Picture of the GAP 50-3-3 heat exchanger [19].

As can be seen in figure 28, ACTE's GAP exchanger are manufactured using a clever mix of pipes and plates, allowing a closed volume in which a liquid can flow and providing a much larger exchange surface for the same length. The main liquid supply pipe before entering in the heat exchanger is divided into three smaller pipes. These three pipes provide the liquid to three collectors and then to the closed volumes. The liquid flows through the annular tubular plates. At the outlet of the heat exchanger the reverse process occurs.



Figure 28. Picture of one side of the GAP 50-3-3 heat exchanger [19].

The gap between the plates, where the hot gas can flow, is 3 mm. Thanks to the combination of performance, reliability and compactness, the GAP-type heat recuperators make waste heat recovery within reach of all industrial processes.

3.2 Test bench description

The main configuration at scale of the test bench is shown in figure 29, and the main components are:

1. centrifugal fan
2. burner
3. mixer
4. flow straightener
5. converging interface duct
6. heat exchanger
7. diverging interface duct
8. chamber
9. nozzle bench
10. discharge duct

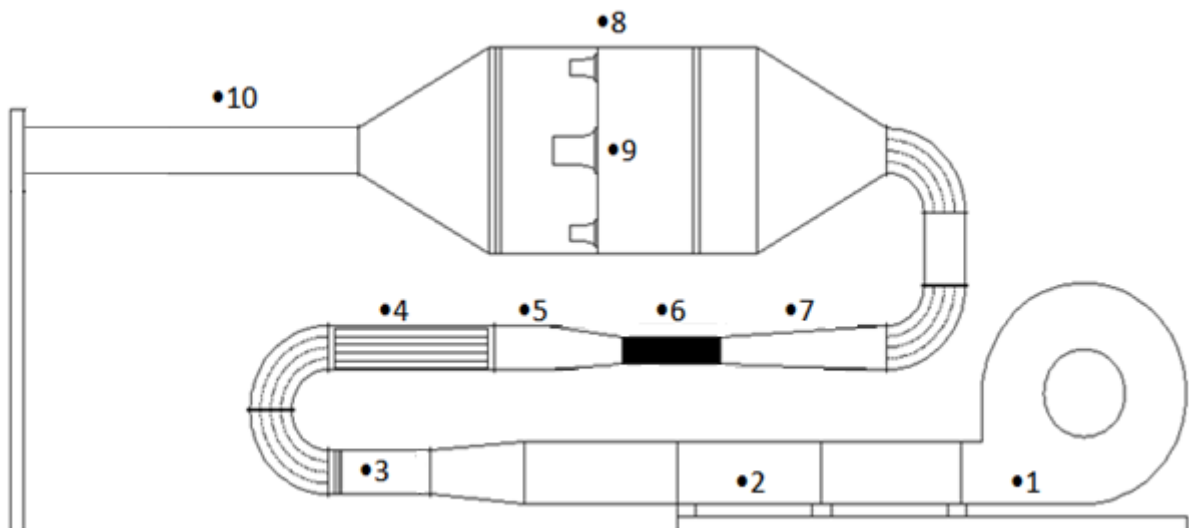


Figure 29. Test bench scheme. 1: centrifugal fan, 2: burner, 3: mixer, 4: flow straightener, 5: converging interface duct, 6: heat exchanger, 7: diverging interface duct, 8: chamber, 9: nozzle bench, 10: discharge duct.

The test bench is divided into three levels. The first level is used for the generation of a stream of hot gas at a uniform temperature. The second level is used to stabilize the flow and test the heat exchanger. The third level is used for the gas mass flow measurement and discharge of the exhaust gas. More information related to the different systems and components of the test bench can be found in the following sections.

Since the test bench is used to test devices to recover waste heat from the exhaust gas of the aeronautic engine test bench, it should be able to provide a stream of hot gas. In this case, atmospheric air is provided to a burner that produces a hot gas stream. The recovery heat exchanger is installed within the exhaust gas mass flow. At the same time, a stream of working fluid is supplied to the recovery heat exchanger. Due to the low cost, safety and high availability, the tests have been performed using water as working fluid. In order to measure the performance of the recovery heat exchanger, the test bench is equipped with measurement instruments.

In order to simplify the test bench design, as well as the experimental procedure, an open loop configuration for both the gas and the working fluid side has been used. The use of a close loop configuration would require the use of a heat dissipation unit, which would increase the complexity of the test bench design in a considerable way.

There is not any phase change of the working fluid within the heat exchanger.

A mass flow like the one that is found in the turbofan and turbojet exhaust is way too large to be reproduced under laboratory conditions. Producing such a large mass flow rate would be impractical and extremely expensive. For that reason, the mass flow of hot gases is going to be scaled. Also the water mass flow rate for the same reasons is going to be scaled. The temperature range of the hot gas flow rate that can be simulated is limited by the burner capacity. The range will be shown in the tests section.

Initially, the hot gas generator, composed by a centrifugal fan and a burner, heats up a stream of air. Next, the stream of hot gas flows through a static mixer to avoid temperature stratification. The stream of exhaust gas will be redirected by means of a curved duct and then it will flow through a flow straightener before its entry to the heat exchanger. Static pressure and temperature measurements will be done before and after the heat exchanger. After leaving the heat exchanger, the gas flow is conducted by means of a

curved duct, through the bench of nozzles where the mass flow rate of the gas flow is measured. Static pressure and temperature measurements will be done before the mass flow measurement. Finally, the gas flow is discharged into the atmosphere.

In order to supply a flow of air through the test bench ducts, the fan has to be able to overcome the pressure drop generated by the ducts and the test bench accessories. The total pressure drop of the test bench can be expressed as the sum of the frictional and the individual pressure drop of all the test bench components.

3.2.1 Hot gas generator

The hot gas generation unit is composed by:

- a centrifugal fan
- an electric motor
- a burner
- a PID control system
- gas and electrical connections

Figure 30 shows a scheme of the hot gas generator.

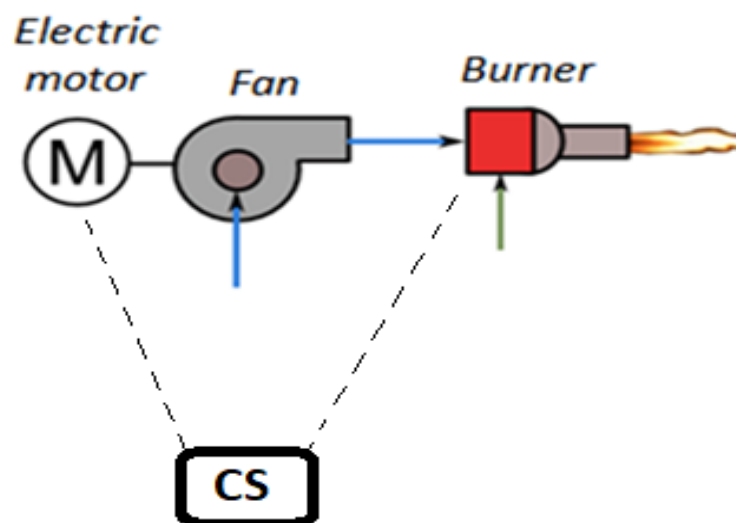


Figure 30. Scheme of the hot gas generator.

Technical drawing of the hot gas generator layout is shown in figure 31.

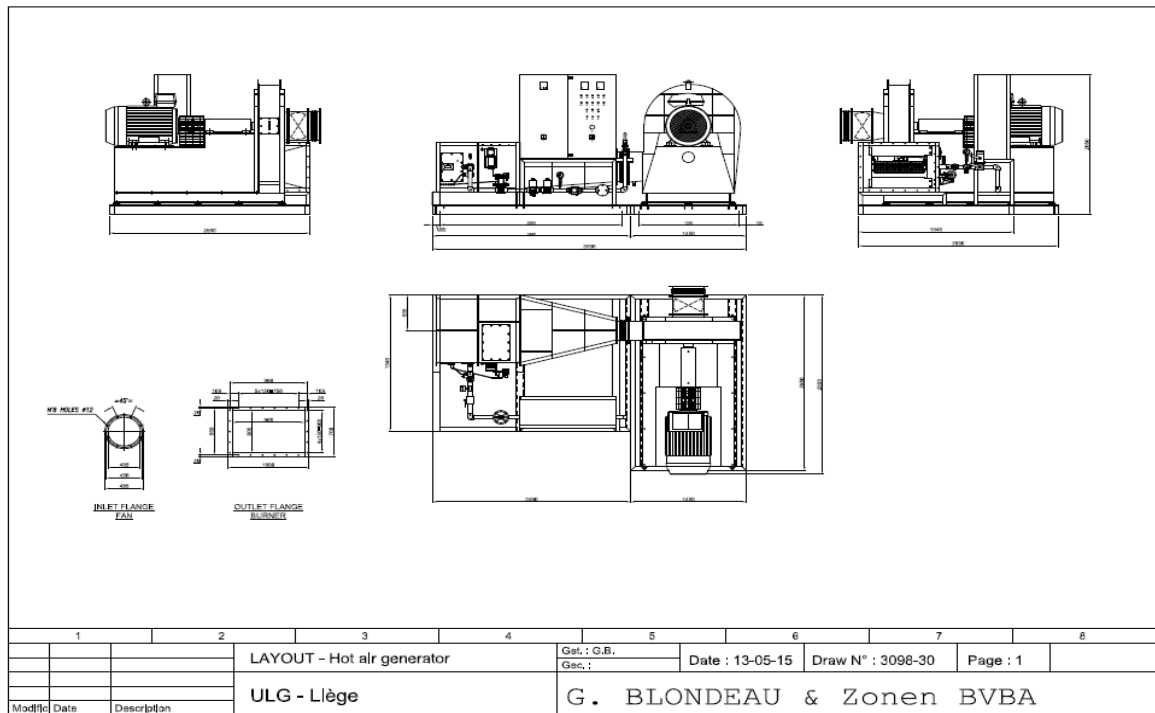


Figure 31. Technical drawing of the hot gas generator layout.

The centrifugal fan, driven by an electrical motor, is used to impulse a desired amount of air to the burner. In order to adjust the air mass flow rate, the electrical motor is provided with a variable frequency drive to modify its rotational speed.

The centrifugal fan is coupled to a burner. The burner maximum power is 350 [kW] and it is placed inside a rectangular duct.

Additionally, the system also counts with a PID control system that is able to adjust the hot exhaust gas temperature automatically, considering the frequency of the centrifugal fan, by changing the power that is being delivered by the burner.

The hot gas generator includes a complete gas train and a gas flow meter. The gas train meets all the of security standards that are required for the operation of the burner.

The electrical energy (3X380 [V]) is provided to the hot air generator by means of cables. A cable of 135 [mm²] and a cable of 4 [mm²] of cross sectional area are used to supply

electricity to the electric motor of the fan and to the rest of the electric devices, respectively.



Figure 32. Hot air generation unit placed in the room where the test bench has been built.



Figure 33. Picture of the burner.

The place where the hot air generator is installed is provided with natural gas at a pressure of 300 [mbar]. In order to supply the gas that is required for the hot gas generator operation, a gas line has been installed. The line has been derived from an existing gas line that has been previously built for another test bench. The line consists in a pipe that conducts the gas from the modified gas connection until the gas connection of the hot gas generator. The new gas line is derived from the existing gas line using a “T” type fitting. Ball valves will be used to isolate the gas line. Figure 34 shows a scheme of the new gas line and the fittings used for its construction.

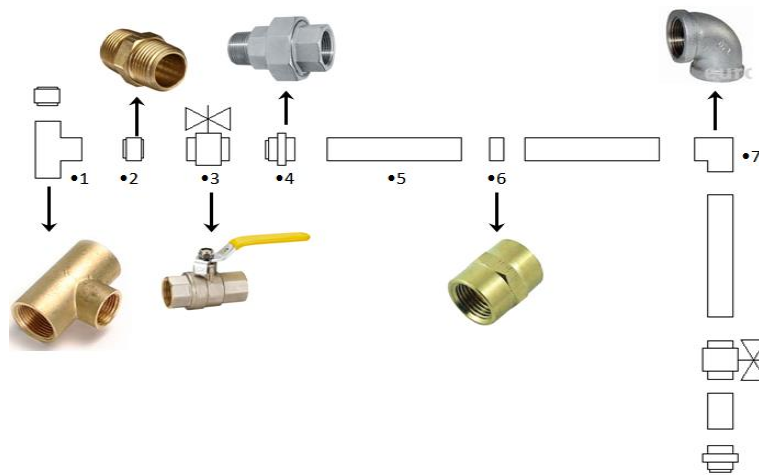


Figure 34. Scheme of the new gas line.



Figure 35. Pictures of a part of the gas line (left) and the material used for the electric connection (right).

3.2.2 The mixer

When the air stream leaves the hot exhaust gas generation unit, it might be stratified in layers of different temperatures, especially in case of mixing cold atmospheric air with hot combustion gas. In order to avoid temperature stratification of the gas stream and obtaining good temperature measurements, a mixing device is used. In general terms a mixer is a device used to obtain a uniform temperature in a stream of fluid.

The design of the mixer was done by the University of Liege and it is based on mixers designs proposed by the ASHRAE (The American Society of Heating, Refrigerating and Air-Conditioning Engineers).

The mixer is a louvered static type. It is considered static because it doesn't have moving parts. It consists in fixed louvers that change the fluid stream direction to produce the mixing between the different temperature layers.

The design consists in three different mixing units. The first one produces a vertical mixing of the air stream by changing the direction of the fluid stream in a vertical way. The second unit is analogous to the first unit, but it produces a lateral mixing of the fluid stream (instead of a vertical one). The last mixing unit uses a combination of vertical and horizontal louvers that generate a swirl effect that enhances the mixing. Figure 36 shows a scheme of the mixer design.

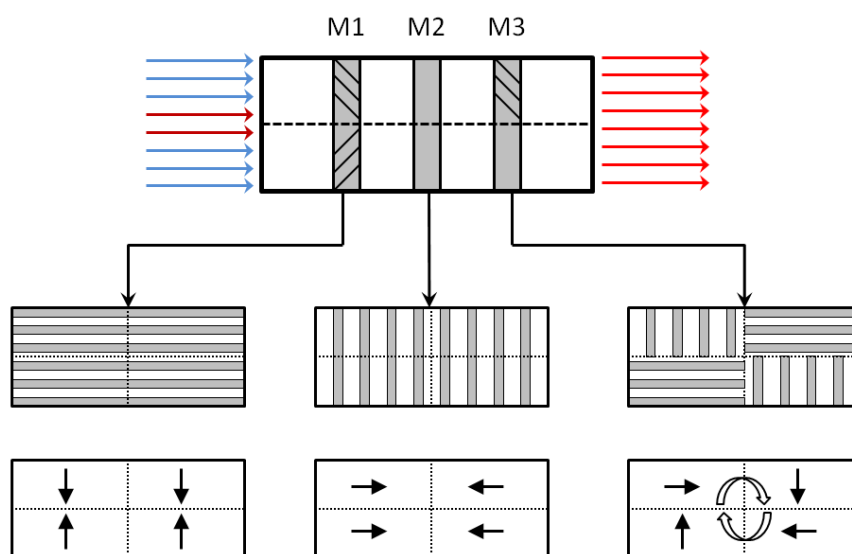


Figure 36. Scheme of the mixer design.

The mixer has been constructed from thin metal plates and it has been fixed inside its corresponding duct by means of welding. In figure 37 is shown a section of the mixer.



Figure 37. Picture of one mixing unit.

3.2.3 Flow straightener

To stabilize the flow, in order to perform quality tests and measurements, is necessary the use of a stabilization length.

In general, the flow stabilization and uniformization is given by allowing the stream to travel along a certain distance, which is a stabilization length. The necessary distance to have a stable flow depends on the types of the elements or accessories placed upstream the measurement or testing devices. The stabilization length is directly proportional to the level of disturbance experienced by the flow. So, if in a test bench there is an accessory which introduces a high level of turbulence, like a mixer for example, the needed stabilization length increases. Figure 38 shows an example of what happens to the velocity profile of a flow before and after the stabilization length.

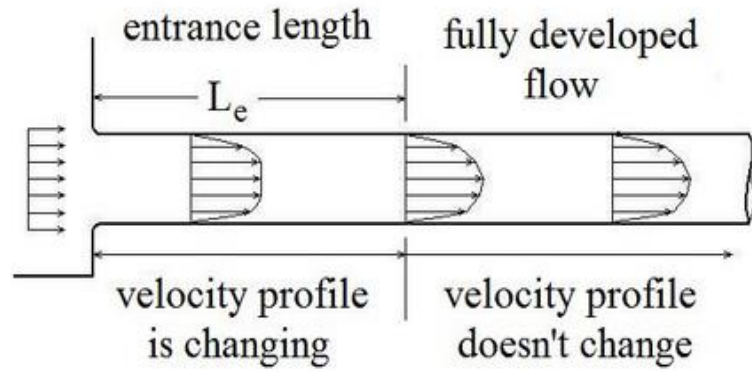


Figure 38. Example illustrating the stabilization length principle.

In the test bench considered, it has been chosen to add the use of a straightener to stabilize the flow. This presents an important advantage: it helps to reduce the stabilization length needed to perform good tests and measurements. The function of a straightener is to produce a virtually uniform velocity of flow. This accessory is able to eliminate eddies and the rotation of the flow produced by the change of direction, due to the test bench configuration, or by the different accessories placed in the stream path.

The type of flow straightener that has been used in the test bench is the tube type flow straightener. When the stream flows through the tubes it is forced to be straightened by the action of the tubes walls. The flow straightener design is based on a design proposed by the ASHRAE and an example is shown in figure 39.



Figure 39. Image of a tube type flow straightener.

The design proposed was adapted to be used in squared section ducts.

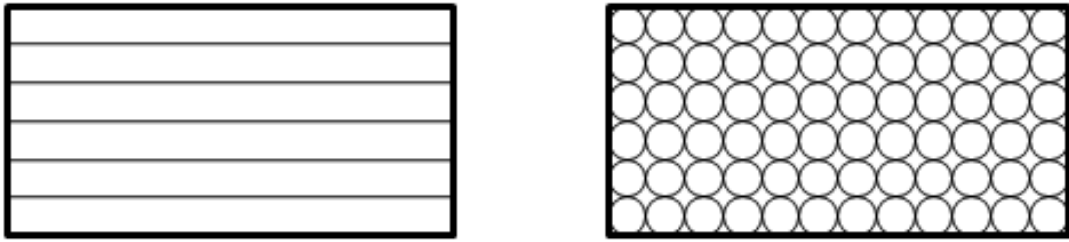


Figure 40. Scheme of the design of flow straightener that is implemented in the test bench.



Figure 41. Tubes and duct used for the flow straightener construction.

3.2.4 Ducts

The test bench includes three different types of ducts: straight ducts, transformation pieces and curved ducts.

The straight ducts are square, rectangular or circular sectioned ducts and they are meant to conduct the flow.

Transformation pieces are used to connect ducts with different cross section. Those pieces consist in a converging or diverging ducts.

The curved ducts are used to change the direction of the flow. These types of ducts are provided with a set of turning vanes, which are sheet metal devices used to smoothly direct the flow where there is a change of direction. The aim of the vanes is to reduce the turbulence and the resistance of the flow that crosses a changing direction duct. So, they decrease the energy loss that the flow experiences when its direction is changed. The vanes of these ducts have been built from thin metal plates that have been curved using rolls. The curved plates have been fixed inside the curved ducts using welding.

Figure 42 shows a scheme of a curved square sectioned duct with turning vanes installed and figure 43 shows a picture of the curved plates (left) and a finished curved duct (right).

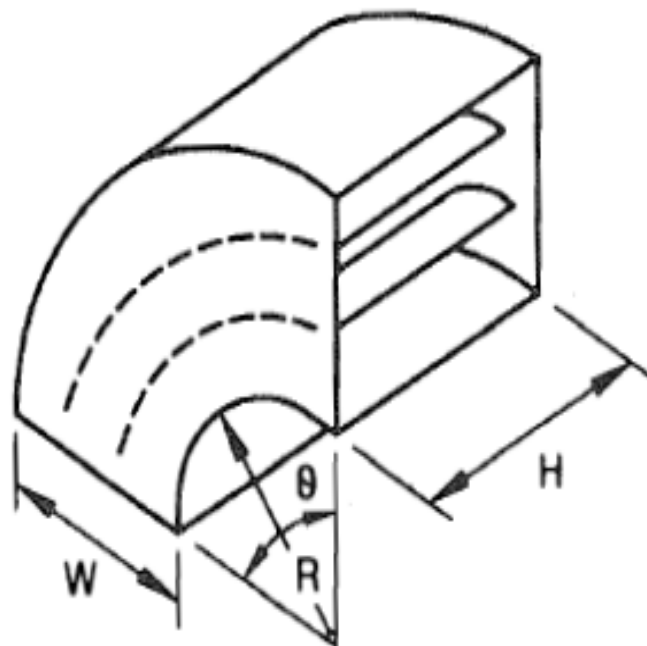


Figure 42. Curved duct with turning vanes.

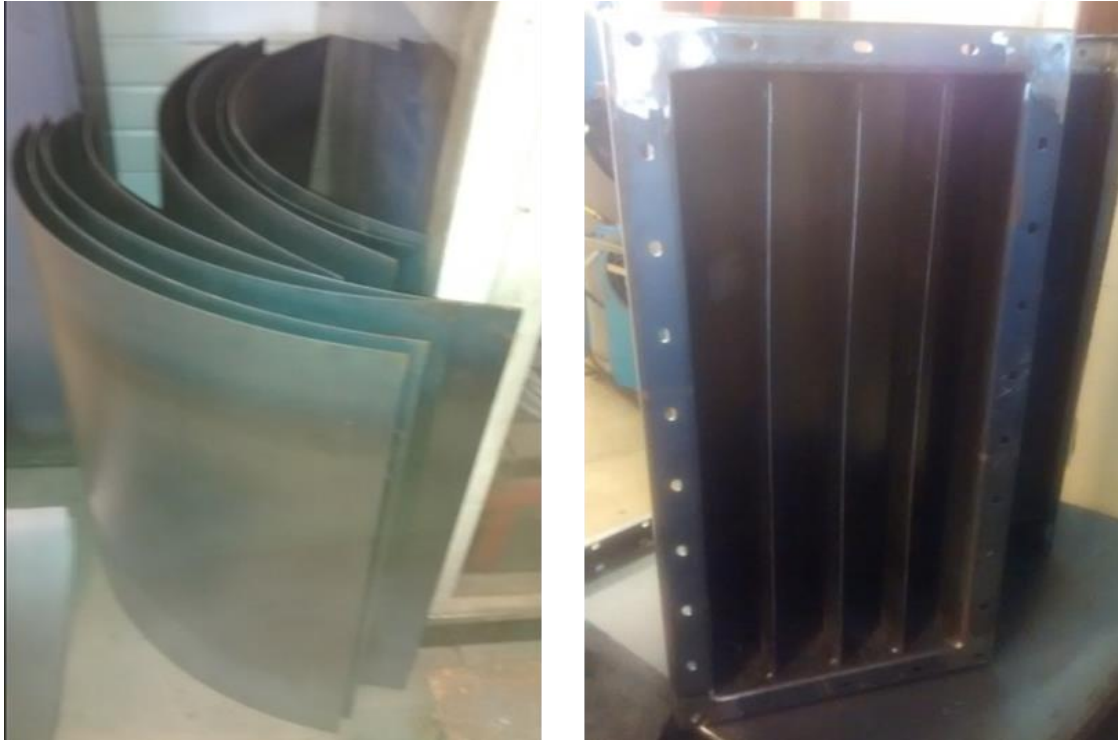


Figure 43. Pictures of the curved plates (left) and the finished curved duct (right).

The length of the ducts has been chosen considering the space limitations of the site where the test bench is built.

The ducts are built in regular steel and the connection between them is performed by means of flanges. The seal between ducts is ensured by the use of bolts and a thermally stable gasket designed for operation at high temperatures.

The entire ducts layout is shown in figure 45 where the numbers represent:

1. straight ducts
2. transformation pieces
3. particular transformation pieces. They have been directly provided by ACTE company



Figure 44. Picture of the transformation duct of ACTE company.

4. curved ducts.

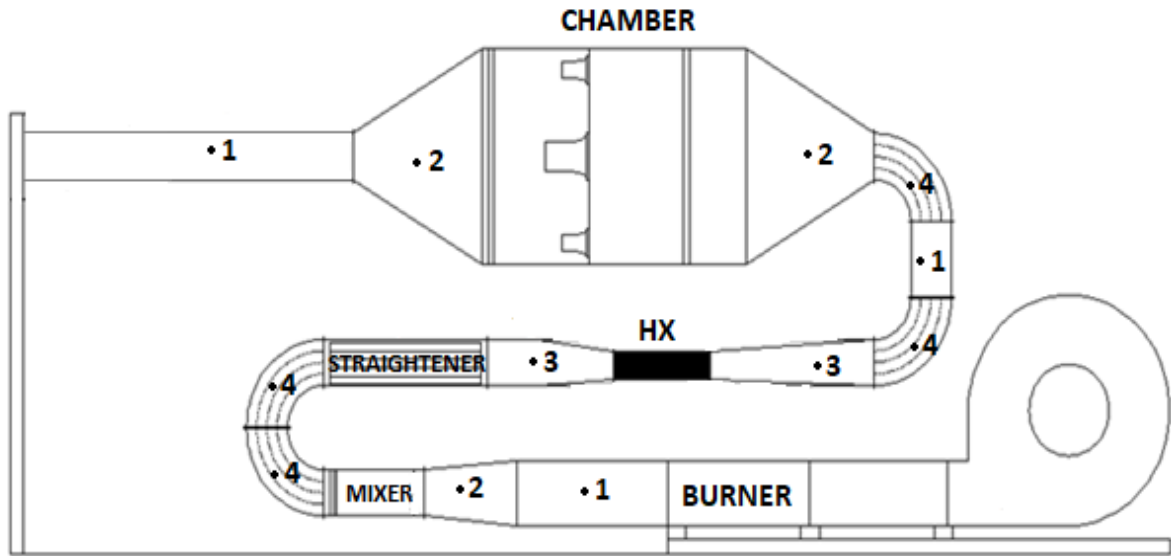


Figure 45. Ducts scheme. 1:straight ducts, 2:transformation pieces, 3:particular transformation pieces, 4:curved ducts.

Figure 46 shows a picture of several of the ducts used for the test bench construction.



Figure 46. Picture of various ducts used for the test bench construction.

3.2.5 Chamber

The chamber is the place where the nozzles, that are required to measure the mass flow rate of the hot gas stream, are located. Its section is considerably bigger than the other ducts used in the test bench construction. This because the aim is to reduce the gas speed. In order to have access to the measurements instruments, a door has been built on the front side. The design of the chamber is based on the AMCA (Air Movement and Control Association International) standards.



Figure 47. Picture of the chamber.

3.2.6 Water loop

The water that is used during the test bench operation is supplied by the water network of the laboratory. The mentioned network is able to provide a maximum flow near to 1,3 [kg/s] at an average pressure of 4 [bar]. The water is conducted to the heat exchanger by means of flexible pipes. The water coming out from the heat exchanger is rejected to the drain of the laboratory.

3.2.7 Support structures

To support the weight of the different components of the test bench, support structures have been built. The structures are able to resist the weight of the test bench components and also to provide a certain degree of freedom to avoid thermal stresses coming from the ducts dilatation.

The first type of support structure consists of a chassis built from steel profiles. This is used to support the ducts placed in the first level of the test bench.

The second type of structure consists of metallic structures that are used to support the weight of the ducts located on the first and the second level of the test bench. The mentioned structures have the shape of an "H", as shown in figure 48. The structures are bolted to the ground and the ducts are free to glide over the structure, avoiding thermal stresses.

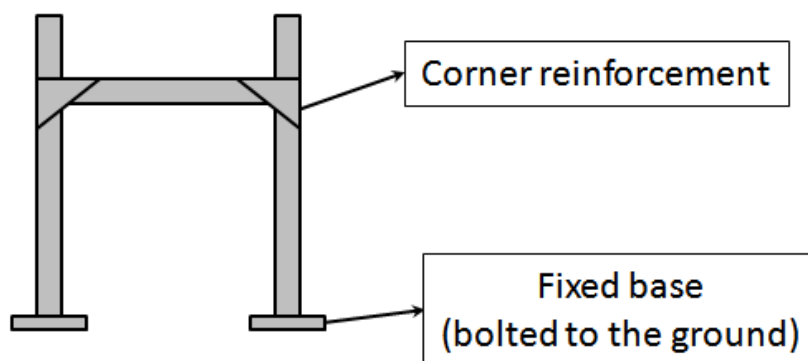


Figure 48. Scheme of the type "H" support used to support the second level of the test bench.

The third level of the test bench is hanging and its weight is supported by chains. The chains have been attached to a set of support beams that have been installed in the room where the test bench has been built.

To increase the safety of the test bench, an additional set of metallic frames were built under the main structure of the chamber, stopping it to fall in case of failure of the

suspension system. This second set of frames is also used to support part of the structure of the second level.

An extraction system has been implemented in the test bench, in order to allow the extraction of the heat exchanger. The system affords to slide the heat exchanger out of the test bench through metal guides.

3.2.8 Thermal insulation

To avoid having the exterior surfaces of the ducts at elevated temperatures and to avoid thermal losses, a layer of insulation has been placed over the outer surface of the ducts. The selected insulation is “Insulfrax” (thermal conductivity: $0,12 \left[\frac{W}{m^2K} \right]$). A layer of 50 [mm] of insulating material has been installed. The insulation counts with an aluminum coating used to protect the thermal insulation and also to avoid the release of fibers of insulation in the air.

Figure 49 shows a picture of the insulating material and an example of the method used for the thermal insulation installation. A metallic strip packing machine was used as fixation system to hold the insulation in place.



*Figure 49. Image of the material used for the thermal insulation of the ducts (left).
Example of the fixation method used (right).*

3.2.9 Measuring instruments

There are three types of measuring instruments throughout the test bench:

1. mass flow rate measuring instruments
2. temperature measuring instruments
3. pressure measuring instruments

3.2.9.1 Mass flow rate measuring instruments

The flow rate of the gas stream is measured by means of nozzles installed within the chamber. The whole gas flow rate is forced to pass through the nozzles. When the stream flows through a nozzle a pressure drop is generated. This happens because the gas accelerates through a nozzle, the velocity increases, the pressure and the gas density decrease. The gas flow rate is determined by measuring the pressure difference at the nozzle inlet and nozzle outlet. Figure 50 shows a scheme of a nozzle flow meter device:

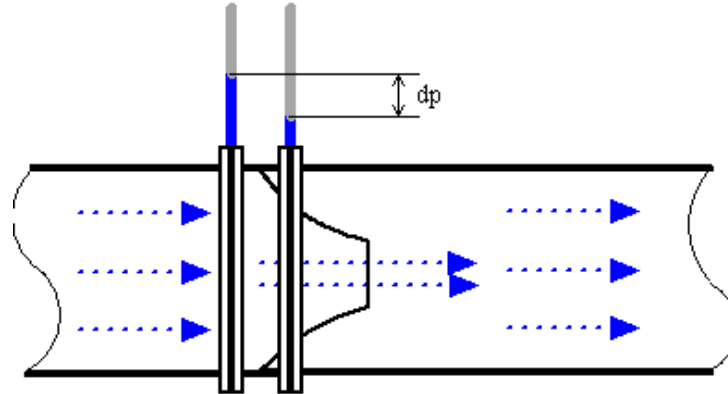


Figure 50. Scheme of the nozzle flow meter device [20].

The design of the nozzles, as well as the relationship between the flow rate and the pressure drop is based in the standard ISO 5167.

To avoid an excessive pressure drop if the tests are performed at high flow rates, or to avoid a little pressure drop if the tests are performed at low flow rates, a nozzles bench has been implemented. A nozzle bench consists in an arrangement of more than one nozzle in

parallel. This type of arrangement allows the adjustment of the pressure drop that is produced. Pressure drop is kept within a desired range by adjusting the number of nozzles and their geometry. The bench of nozzles is installed inside the chamber. The nozzles are attached to a perforated fixation plate using rivets and bolts. Additionally, a set of removable plugs were constructed to cover the entry of some nozzles, allowing the regulation of the generated pressure drop for different gas mass flows.

Figure 51 shows on the left an image of the metallic nozzles used and on the right an image of the metallic nozzles attached to the perforated fixation plate.



Figure 51. Images of the metallic nozzles used and the nozzles attached to the perforated fixation plate.

A settling plate used to settle down the gas flow has been implemented with the nozzles bench inside the chamber. The settling plate consists in a steel plate with circular perforations. Figure 52 shows the settling plate.



Figure 52. Picture of the perforated plate used as settling mean.

For the measure of the water flow rate, the water loop has been equipped with a volumetric water meter.

3.2.9.2 Pressure measuring instruments

Static pressure measurements are done upstream and downstream of the heat exchanger and of the flow rate measuring device (the bench of nozzles). Pressure sensors are used to perform the measurements. In addition to the local pressure measurements, the differential pressure measurements between the inlet and the outlet of the mentioned devices are performed. For pressure measurements, pressure taps have been installed and connected to the pressure transducers. Figure 53 shows a picture of some the pressure taps.



Figure 53. Picture of the pressure taps installed.

Figure 54 shows a picture of the absolute pressure sensors and figure 55 shows a picture of the differential pressure sensors that has been used during the experimental campaign. The absolute pressure sensors have an accuracy of $\pm 1,5\%$. The differential pressure sensors present an accuracy of $\pm 0,5\%$.



Figure 54. Picture of the absolute pressure sensors.



Figure 55. Picture of the differential pressure sensors.

3.2.9.3 Temperature measuring instruments

Thermocouples type-K are used to measure the temperatures through the test bench. To obtain a good accuracy, all the thermocouples used have been calibrated individually. Furthermore, 9 thermocouples have been used for every measuring point. The thermocouples were welded to an electronic card that is part of the data acquisition system. Figure 56 shows a picture of the thermocouples connected to the electronic card.

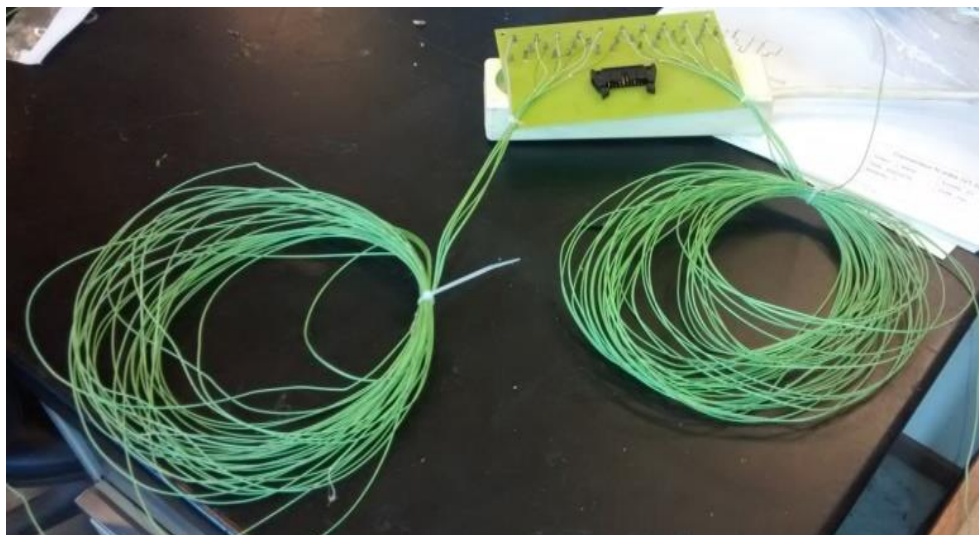


Figure 56. Picture of the thermocouples connected to the electronic card.

It is important to mention that a cold source of water and ice, placed inside an isolated little tank, has been used as a reference temperature at 0 [°C].

The accuracy of the thermocouples is ± 1.1 [K].

3.3 Experimental results

In this section the experimental results will be discussed. All the electrical signals have been acquired and then converted to physical values by a data acquisition system.

Figure 57, figure 58 and figure 59 represent the cartography, which is the measuring range where the tests have been performed.

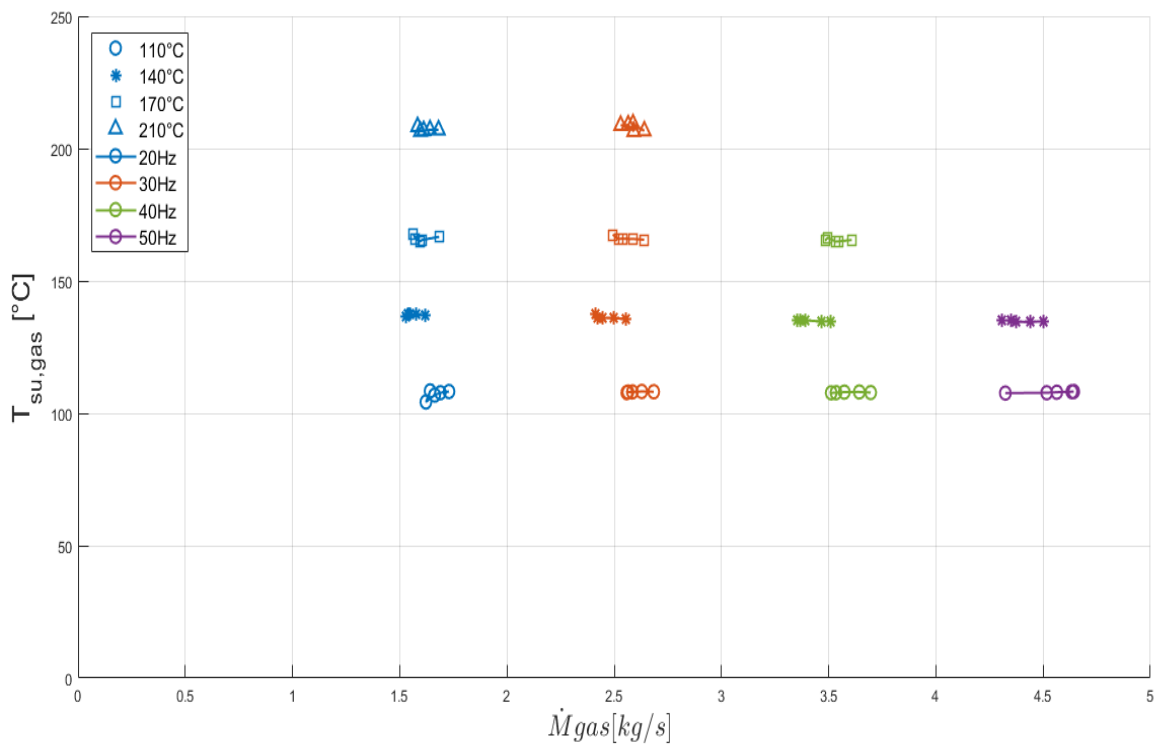


Figure 57. Gas flow rate and temperature tests range.

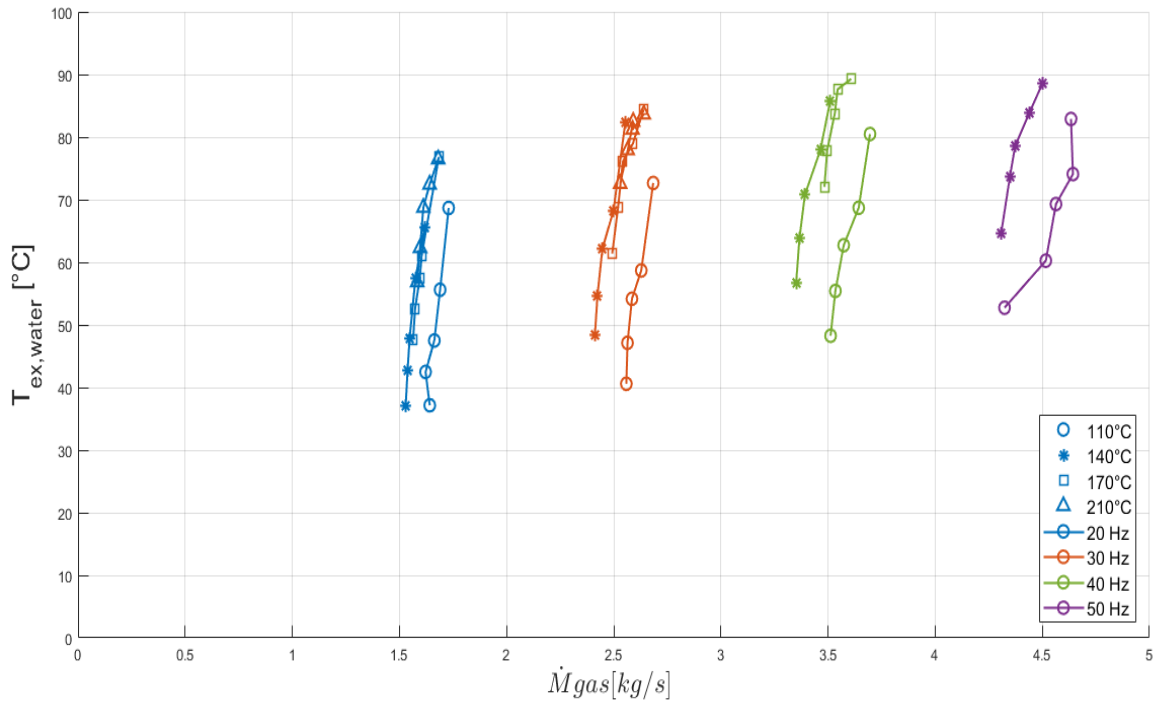


Figure 58. Gas flow rate, temperature range and different water flow rate.

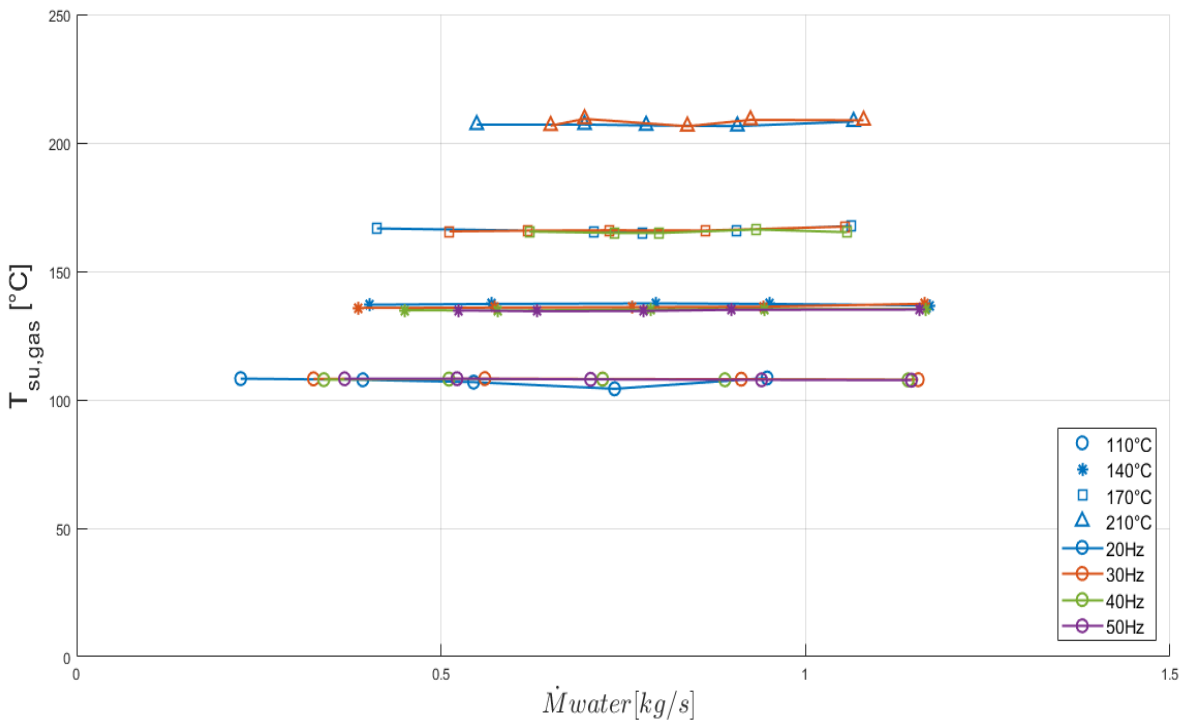


Figure 59. Water flow rate and temperature range.

For all graphs different colours mean different frequencies of the electrical motor and so different speed rotation. It means different air flow rate provided to the burner and so different exhaust gas flow rate at the outlet of this. The frequencies used to perform the test are:

- 20 [Hz]
- 30 [Hz]
- 40 [Hz]
- 50 [Hz]

The shapes of the symbols represent different exhaust gas temperatures at the outlet of the burner and at also the inlet of the heat exchanger:

- 110 [°C]
- 140 [°C]
- 170 [°C]
- 210 [°C]

Furthermore, is possible to see especially from figure 57 and figure 58 that for the higher frequencies some temperature tests are missing because of the power limitation of the burner at 350 [kW]. Under an exhaust gas temperature of 100 [°C] the hot gas generator system was not stable enough to perform tests.

Figure 59 shows the tests range for the water mass flow rate. On the Y-axis $T_{su_{gas}}$ indicates the gas temperature at the inlet of the heat exchanger.

In Figure 58 \dot{m}_{gas} is the gas mass flow rate and $T_{ex,water}$ indicates the water temperature at the outlet of the heat exchanger. Considering one frequency and one exhaust gas temperature at the inlet of the heat exchanger, so one colour and one shape, the highest point of the considered line correspond to the minimum value of the water flow rate used in the test and lowest one to the maximum. In fact, the water temperature at the outlet of the heat exchanger, once the gas temperature and flow rate remain constant at the inlet, decreases if the water flowrate increases.

So in conclusion, a wide range of operating conditions has been reached to study the performances of the heat exchanger.

In order to better understand the differences of the heat transfer rates between the water side and the gas side through the heat exchanger is useful to analyse the graph of figure 60.

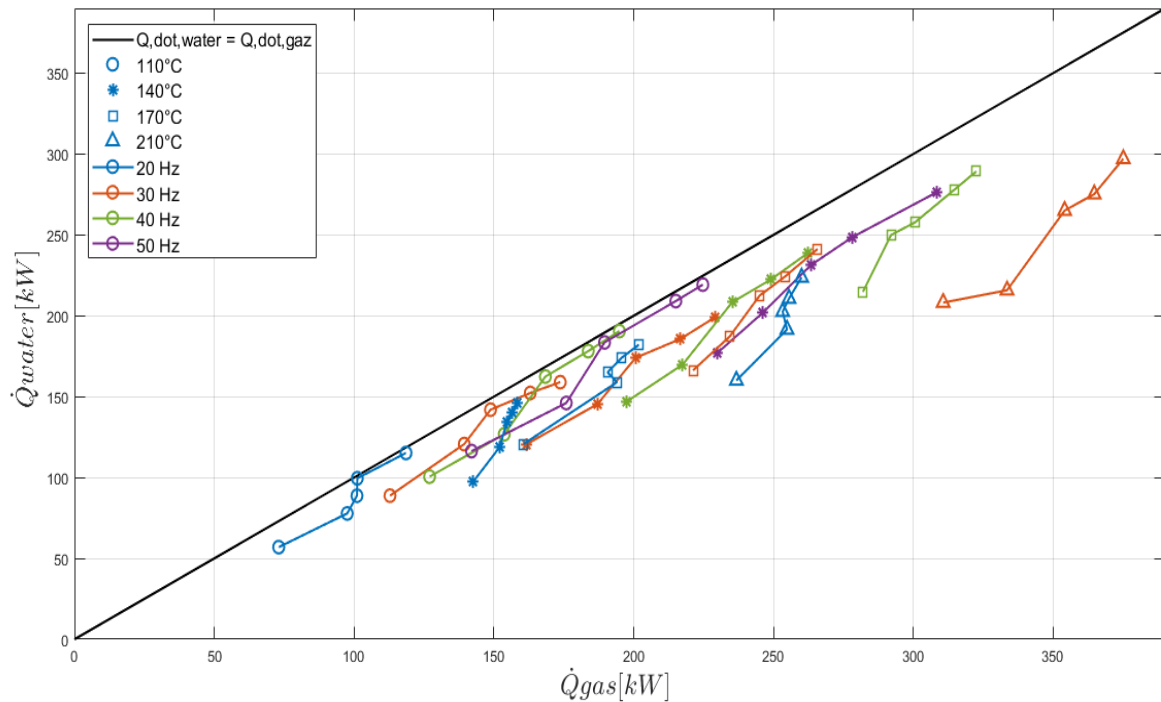


Figure 60. Heat transfer rates of the gas and the water side of the GAP heat exchanger.

The bisector is an indication of the perfect heat exchange between the water flow rate and the gas flow rate. In fact, ideally, the gas side heat transfer rate is equal to the water side heat transfer rate. Actually, due to the heat losses with the environment, the heat transfer rates are different, and this is why the lines do not match up with the bisector.

Considering a single line, so for a fixed gas temperature at the inlet of the heat exchanger and a fixed flow rate, the water flow rate changes from the minimum, on the left of the graph, to the maximum on the right. It is possible to see that with the increase of the water mass flow rate, the line approaches the bisector. This can be explained by the reduction of the environment losses since if the water flow rate increases, the mean water temperature diminishes. This happens because these losses depend on the temperature difference between the water and the environment:

$$\dot{Q}_{loss} = UA \cdot (T_{mean_{water}} - T_{environment}) \quad (43)$$

Where:

U is the overall heat transfer coefficient and A is the heat transfer surface area.

Since all the parameters of the equation remain constant, if $T_{mean_{water}}$ decreases, \dot{Q}_{loss} decreases too.

The relation between the heat transfer rates is expressed as:

$$\dot{Q}_{water} = \dot{Q}_{gas} - \dot{Q}_{loss} \quad (44)$$

Finally, from this equation it is possible to see that if the heat losses decline the difference between the heat transfer rates decrease.

Another important consideration can be done for a fixed water flow rate. In fact, it is possible to notice that with the rise of the gas temperature at the inlet of the heat exchanger or with the increase of frequency, the heat losses to the environment grow. So, the points in the graph deviate from the bisector more and more.

The tests performed gave also the chance to evaluate the pressure drops along the gas and the water sides of the GAP heat exchanger. The pressure drops trends are shown in figure 61 and in figure 62.

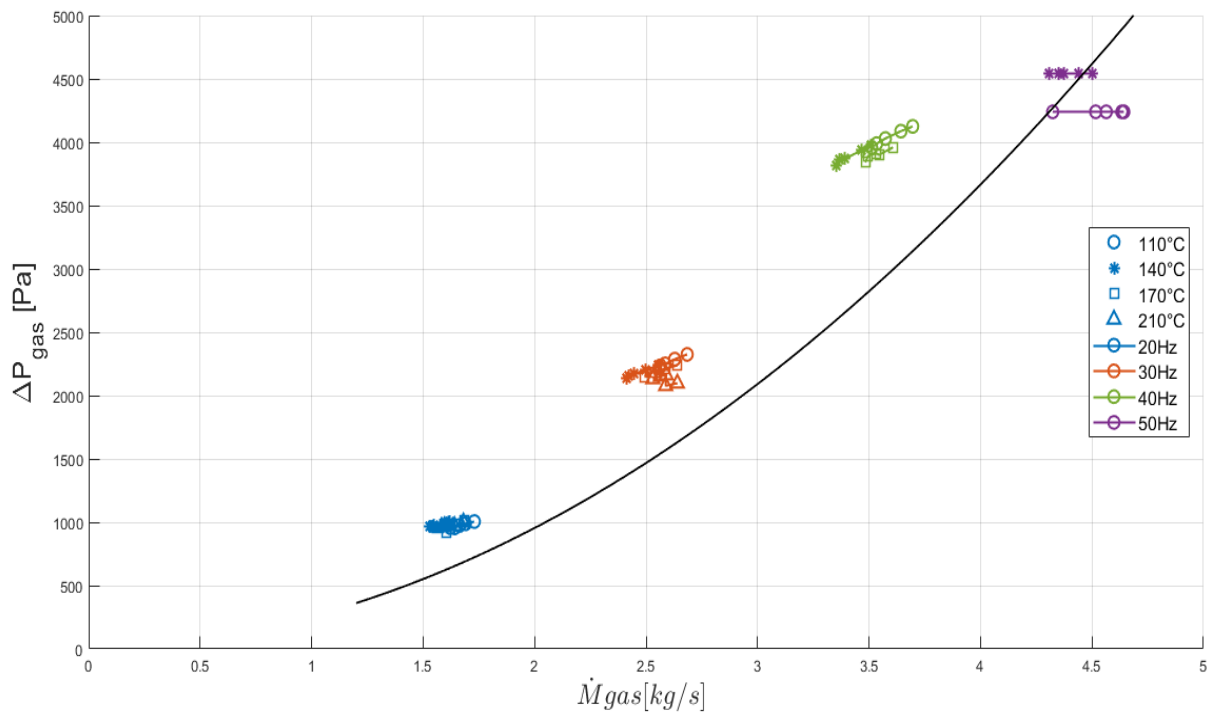


Figure 61. Pressure drops throughout the gas side of the GAP heat exchanger.

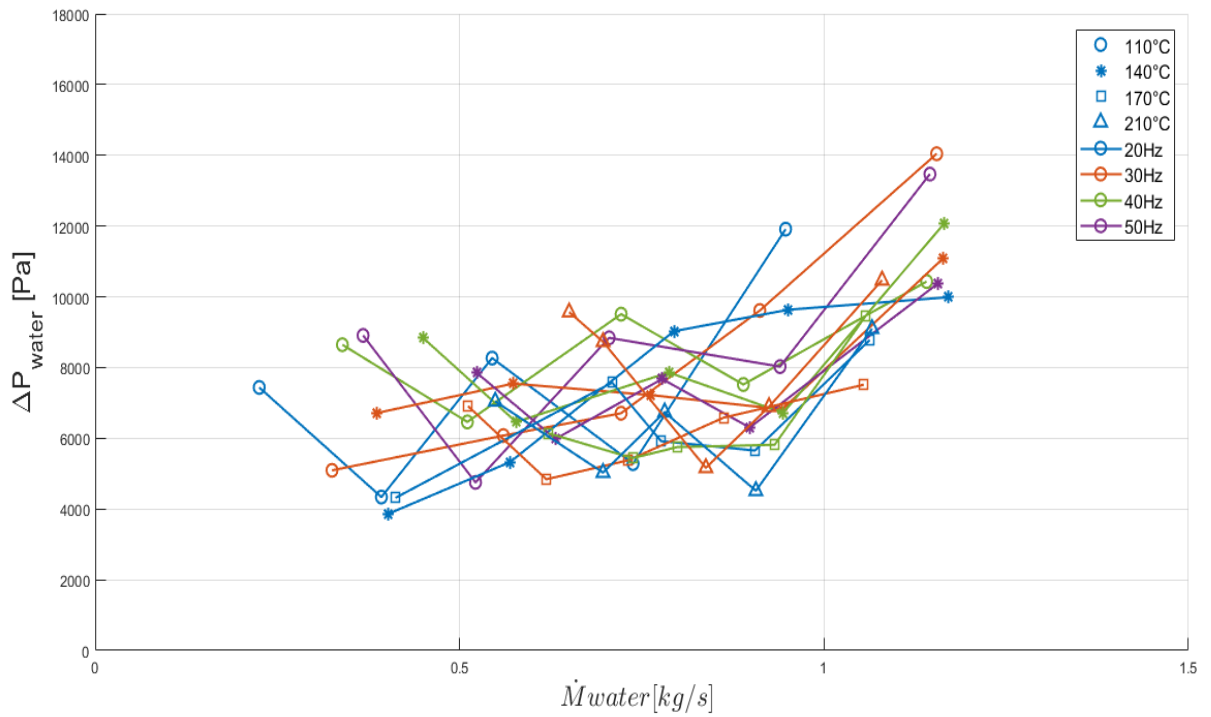


Figure 62. Pressure drops throughout the water side of the GAP heat exchanger.

The pressure drops trend at the gas side, in figure 61, is compared to the one given by ACTE company, which is represented by the black line. The results of the tests show a very similar trend. The pressure drops depends on a parabolic law of the gas mass flow rate.

The measured pressure drop is relatively low and proves that the design of the heat exchanger has been well done.

For the water side, figure 62, the trend of the pressure drops is not clear as the one of the gas side. Generally, looking at coloured lines all together as a mean, it is possible to see that it also follows a parabolic law. The pressure measurement may be affected by two factors. The main one consists in the pressure sensors, used to measure the pressure at the inlet and at the outlet of the heat exchanger, are absolute ones. Instead the pressure measurement for the gas side are both absolute and relative. The minor accuracy of the absolute one can explain in part some strange deviations. The other reason of the imprecise trade can be find in a moving pressure of the water provided by the laboratory network. Due to the fact that too many utilities through the laboratory are supplied by the same network, the pressure in the water circuit have some swings.

Eventually, one of the most important aspects, to evaluate the performances of a heat exchanger, has been tested: the efficiency.

The efficiencies of the gas side are different from the one of the water side because of the heat transfer rates, as seen before, is not the same due to the environment heat losses(43)(44). The lower effectiveness belongs to the water side, because of a lower heat transfer rate.

This can be seen also from the following equations:

$$\varepsilon_{HX_{water}} = \frac{\dot{Q}_{water}}{\mathbf{Min} [\dot{C}_{water}; \dot{C}_{gas}] \cdot (T_{su_{gas}} - T_{su_{water}})} \quad (45)$$

$$\varepsilon_{HX_{gas}} = \frac{\dot{Q}_{gas}}{\mathbf{Min} [\dot{C}_{water}; \dot{C}_{gas}] \cdot (T_{su_{gas}} - T_{su_{water}})} \quad (46)$$

Where:

- $T_{su_{gas}}$ is the gas temperature at the inlet of the heat exchanger,
- $T_{su_{water}}$ is the water temperature at the inlet of the heat exchanger,

- $\text{Min} [\dot{C}_{water}; \dot{C}_{gas}]$ represents the minimum value between \dot{C}_{water} and \dot{C}_{gas} already defined in the first chapter (1) (2).

The denominator is equal for both sides, but as shown previously $\dot{Q}_{gas} > \dot{Q}_{water}$, so $\epsilon_{HX_{water}} < \epsilon_{HX_{gas}}$.

Figure 63, figure 64 and figure 65 show three graphs with different view of the water side efficiency, while varying the gas and the water mass flow rates and the temperature of the exhaust gas at the inlet of the GAP heat exchanger.

The efficiency range, for the tests performed, goes from a minimum value around 0,4 to a maximum value around 0,75.

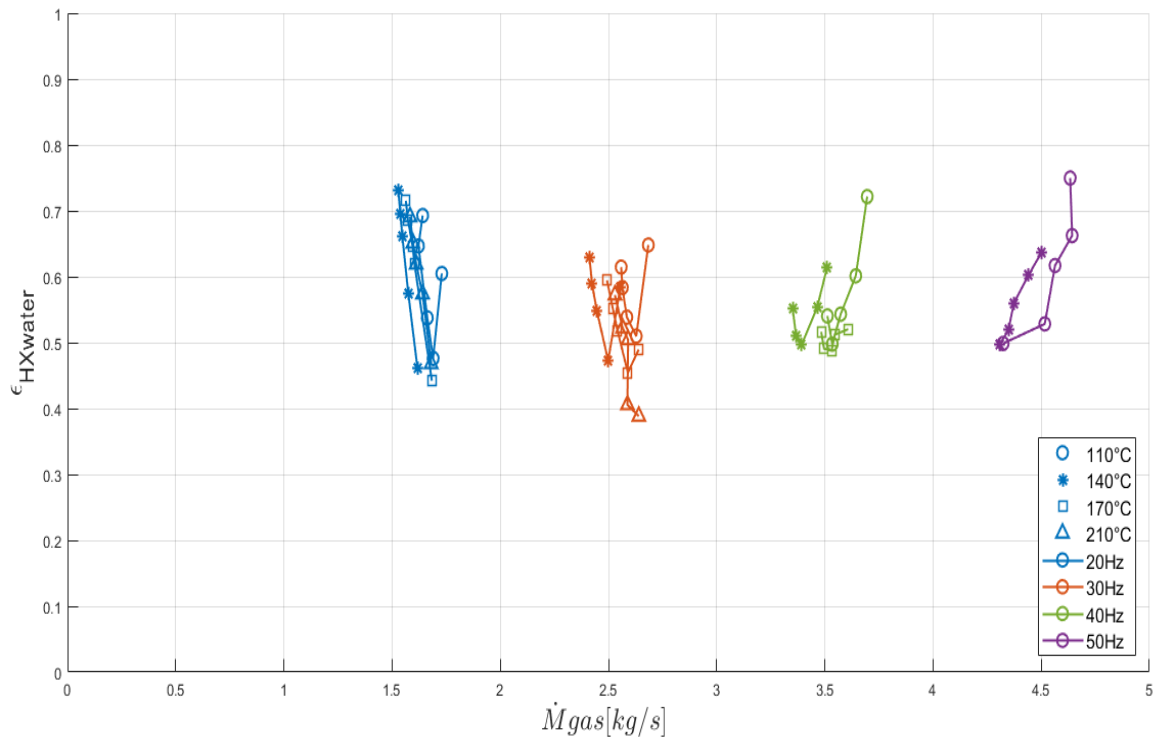


Figure 63. Efficiency of the water side in function of the gas mass flow rate.

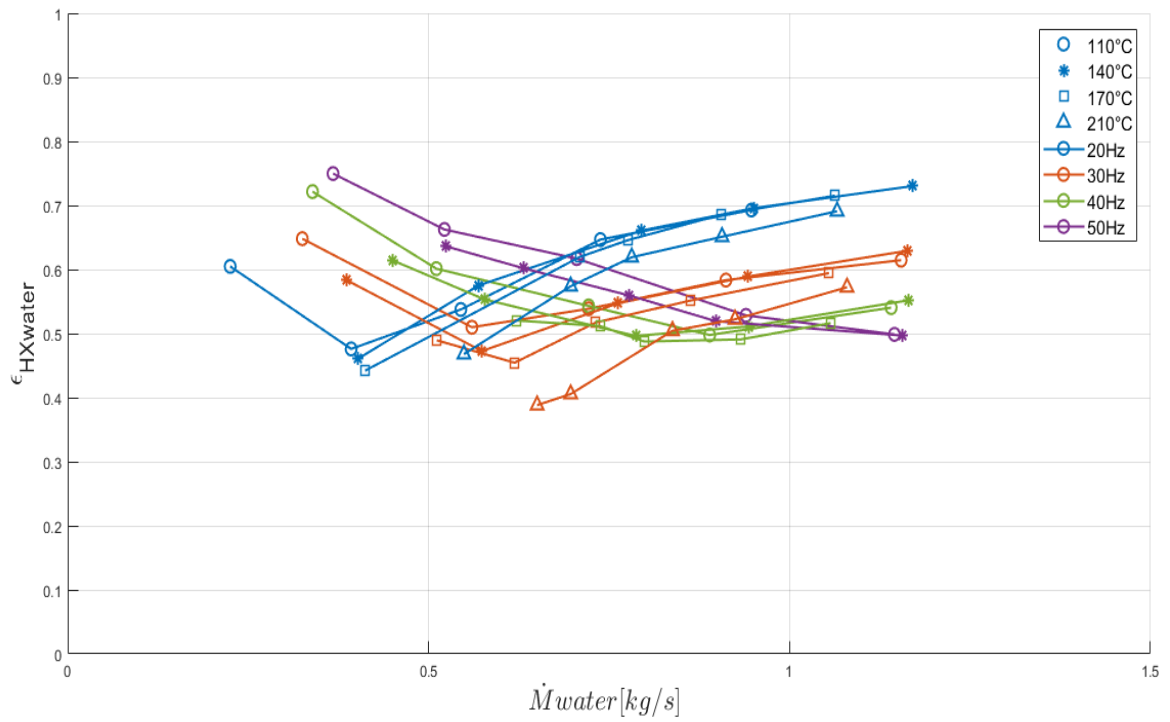


Figure 64. Efficiency of the water side in function of the water mass flow rate.

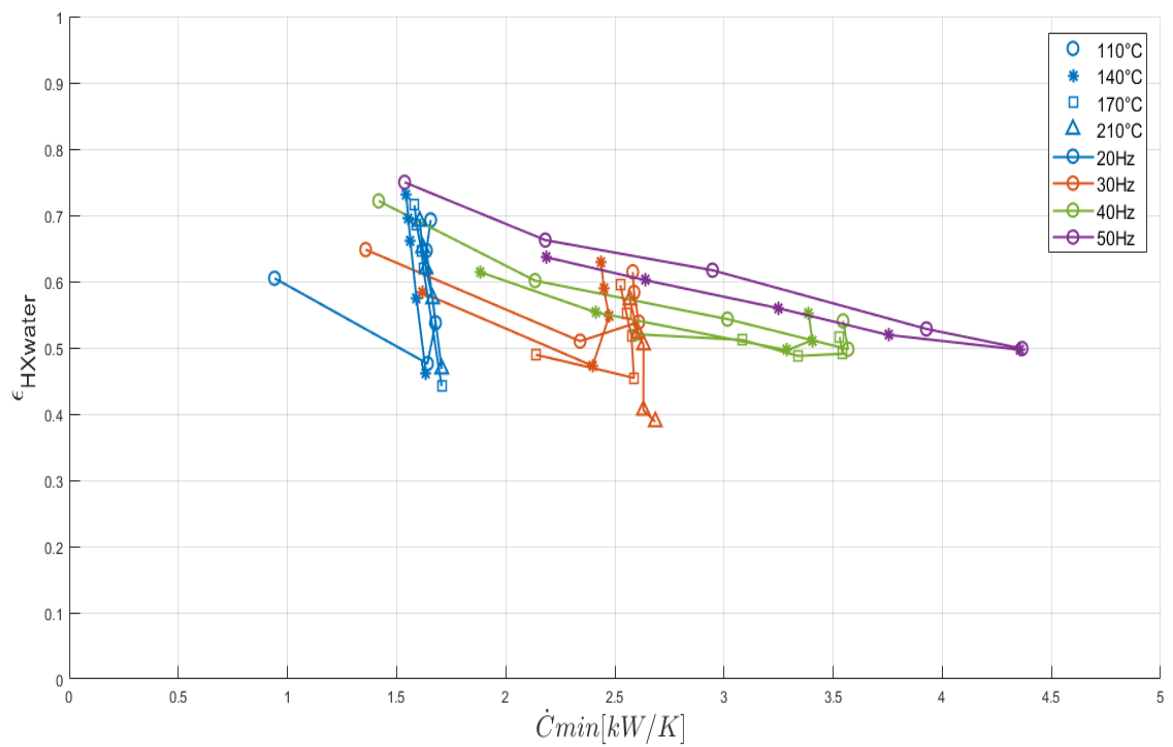


Figure 65. Efficiency of the water side in function of the \dot{C}_{min} .

From figure 64 it is possible to distinguish two different trade of the efficiency:

- For 20 [Hz] and 30 [Hz] the effectiveness increases if the water mass flow rate rises
- For 40 [Hz] and 50 [Hz] the effectiveness decreases if the water mass flow rate rises

This happens because of the \dot{C}_{min} .

For low frequencies (20 [Hz] and 30 [Hz]) \dot{C}_{min} corresponds to \dot{C}_{gas} and so remains constant while varying the water flow rate during a single frequency test. Considering the previous formula (45) of the water side effectiveness, the denominator remains constant while the numerator increases with the rise of the water flow rate, as shown before.

For high frequencies (40 [Hz] and 50 [Hz]) \dot{C}_{min} corresponds to \dot{C}_{water} , which grows with the rise of the water flow rate.

Figure 10 represent the trade of \dot{C}_{water} and \dot{C}_{gas} while varying the frequency for a fixed temperature. Particularly, the graph shows the tests for a temperature of 110 [°C].

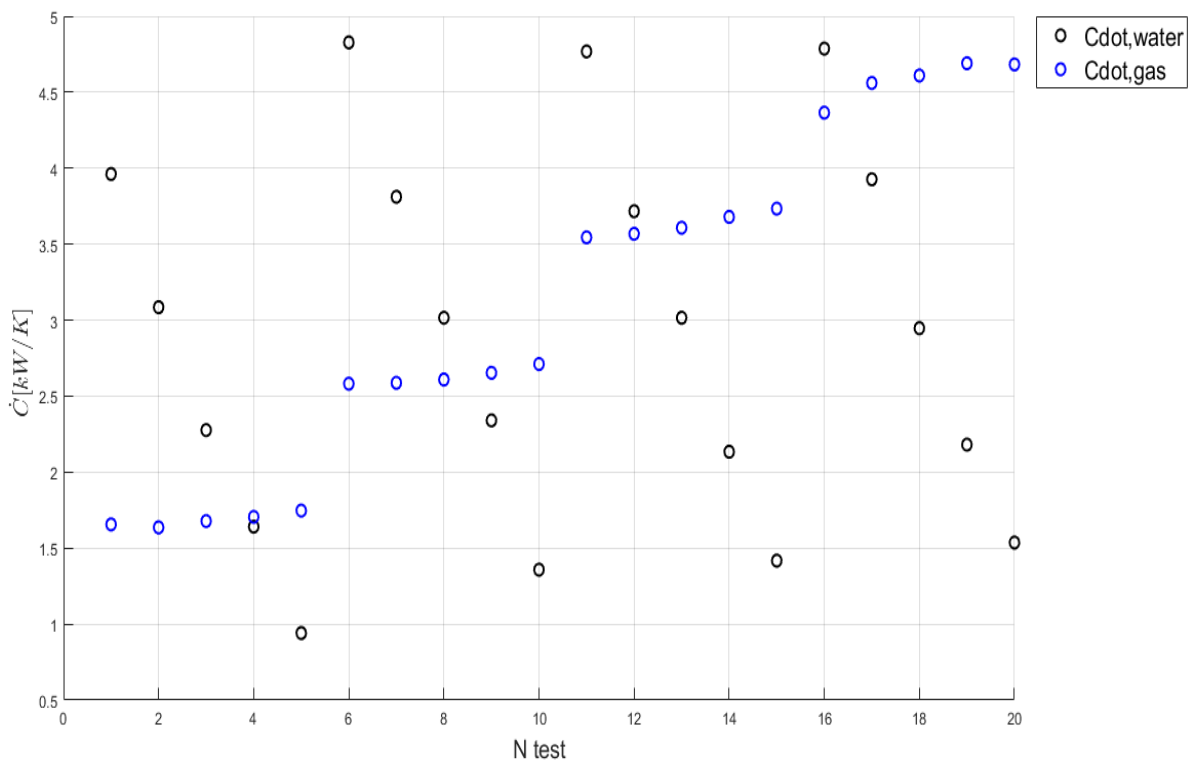


Figure 66. Trade of \dot{C}_{water} and \dot{C}_{gas} while varying the frequency.

The first 5 tests were performed with a frequency of 20 [Hz], the ones between 5 and 10 with a frequency of 30 [Hz], the last two tests with 40 [Hz] and 50 [Hz].

3.4 Conclusions

In this section will be presented the conclusions about the techno-economic and the experimental investigations.

3.4.1 Techno-economic investigation conclusions

In light of the results of the payback time calculation, which is one of the most important criteria to evaluate the GO/ NO GO decision of the implementation of a waste heat recovery system in the test benches, the use of the two systems investigated to recover energy don't represent feasible solutions in some cases for both sites. This conclusion is based on the general minimum payback time criteria adopted by the industrial companies.

The main reasons, which can explain the payback time results, are the limitation in terms of the temperature that the tank can achieved, the cost of the investments quite high and too low engine test hours compared to the building heating need.

Furthermore, the water tank volume has a huge impact on energy savings that can be achieved in the turbojet boiler solution because of the temperature limitation. Since not all the available heat is recovered due to the tank limitation, it should be better to consider less efficient but cheaper heat exchanger in order to decrease the total investment and thus reduce the payback time.

Considering the Norway site, the possibility to produce electric energy from hot exhaust gas, including an ORC (Organic Rankine Cycle) system, could be an interesting future case study. By this way could be possible to recover all the waste heat because there would not be any temperature, and so energy recovered, limitations.

The boiler solution represents in most cases the best system from the payback time point of view. The heat pump solution payback time is strongly related to the difference between the fuel and the electricity price, as primary sources.

Another important aspect to take into account in the techno-economic investigation is, as mentioned in the introduction, the pollution reduction. Both the solutions proposed for the waste heat recovery for heating purposes are environmentally friendly. They allow to reduce the global emissions of the test benches buildings and also the temperature of the exhaust gases before being discharged to the atmosphere. So, for this reason the feasibility of the investigated solutions must not be limited to an economic point of view, but it has to consider also the positive environmental aspects.

3.4.2 Experimental investigation conclusions

A test rig has been used to characterize the performance of a new type of heat exchanger specially designed for waste heat recovery purposes. The GAP 50-3-3 heat exchanger has been tested for a wide range of operating conditions, according to the limits imposed by the test bench components.

The main conclusions, deductible from the performed tests:

- there are high ambient losses up to 30 %
- decent efficiency up to 75%
- low gas and water pressure drops

Such a heat exchanger could be useful to recover waste heat efficiently in every field of industry, at relatively low cost.

3 Bibliografia

- [1] A. Barbotin, R. Cervi, O. Delabroy, G. Gouefelec e C. Lebrun, «Performance enhancement of reheating furnaces using oxycombustion.,» in *AISE Annual Covention*, Chicago, 2000.
- [2] A. Foresti, D. Archetti e R. Vescovo, ORCs in steel and metal making industries: lesson from operating experience and next steps, Dusseldorf, Germany: METEC & ESTAD, 2015.
- [3] G. Bonvicini, Heat recovery potentials in the most demanding processes, 2015.
- [4] United States Air Force, “www.shaw.af.mil,” [Online]. [Accessed January 2018].
- [5] Micro Finish Engineering Co, “www.microfinishengineering.com,” [Online]. [Accessed November 2017].
- [6] ACTE, «Heat exchangers thermodynamical sizing,» 2013.
- [7] “www.dow.com,” [Online]. [Accessed October 2017].
- [8] A. Bolher, R. Casari, E. Fleury, D. Marchio e J. Millet, Méthode de calcul des consommations d’énergie des bâtiments climatisés "consoclim. Ecole des Mines (Paris)., 1999.
- [9] P. Rivière, Performances saisonnières des groupes de production d’eau glacée. Thèse de doctorat. Ecole des Mines de Paris., 2004.
- [10] S. Gendebien, F. Ransy, E. Georges e V. Lemort, «Création d’une base de données de paramètres pour modèles de pompes à chaleur résidentielles. Projet FlexiPAC.,» 2014.
- [11] “www.degreeedays.net,” [Online]. [Accessed October 2017].
- [12] “www.rets-project.eu,” [Online]. [Accessed October 2017].
- [13] “www.elgas.co.nz,” [Online]. [Accessed October 2017].

- [14] J.-C. Hadorn, «Storage solutions for solar thermal energy,» 2004.
- [15] D. Pearson e P. Nellissen, «Application of industrial heat pumps,» 2012.
- [16] “www.ec.europa.eu,” [Online]. [Accessed October 2017].
- [17] “www.mazout-on-line.be,” [Online]. [Accessed October 2017].
- [18] “www.mylpg.eu,” [Online]. [Accessed October 2017].
- [19] “www.acte-sa.be,” [Online]. [Accessed November 2017].
- [20] “www.globalspec.com,” [Online]. [Accessed February 2018].